Effect of interactions on the topological expression for the chiral separation effect

M. A. Zubkov[*] and Ruslan A. Abramchuk[†]

Physics Department, Ariel University, Ariel 40700, State of Israel

(Received 19 February 2023; accepted 18 April 2023; published 16 May 2023)

In the absence of interactions the conductivity of the chiral separation effect (CSE) in the system of massless fermions is given by a topological expression; interactions might change the pattern drastically. However, we prove that the CSE conductivity is still given by the topological invariant composed of the Green functions at zero temperature as long as the chiral symmetry is present, and if the renormalized axial current is considered. This allows us to predict its appearance with the standard value of conductivity per the Dirac fermion $\sigma_{\mathrm{CSE}} = \frac{1}{2\pi^2}$ in quark-gluon matter at $T = 0$ and sufficiently large baryon chemical potential, in the hypothetical phase with restored chiral symmetry and without color superconductivity. This phase may be realized inside the neutron stars. We also argue that the same topological expression for the CSE may be observed in Weyl semimetals, which realize the system of interacting relativistic fermions in solid state systems. In order to estimate the nonperturbative corrections to σ_{CSE} within QCD at finite temperatures we apply the method of field correlators developed by Yu. A. Simonov. As expected, above the deconfinement crossover, the topological expression is approached within the quark-gluon plasma phase, when the quark chemical potential is sufficiently large. However, we observe that this occurs only when quark chemical potential is much larger than the thermal (Debye) mass. This range of parameters appears to be far out of the region accessible at the modern colliders.

DOI: 10.1103/PhysRevD.107.094021

I. INTRODUCTION

The nondissipative transport effects appear in both condensed-matter and high-energy physics [1–14]. These effects represent an important probe of the corresponding systems because of their topological nature. The corresponding conductivities, as expected, in many cases are represented by the topological invariants robust to any smooth modifications of the systems including switching on interactions. As a result, the strong interactions which cannot be taken into account using direct calculations, do not have any effect on these quantities. An example is given by QCD at finite baryon-chemical potential. Here the lattice numerical simulation cannot be applied, while the nonperturbative effects still remain essential. In particular, the appearance of color superconductivity predicted with the aid of perturbative QCD is questionable because of the nonperturbative nature of QCD even at large μ_B.

The sketch of the phase diagram of QCD is represented in Fig. 1 in the plane temperature-quark chemical potential [6,15–24]. The vacuum of the theory ($T = \mu = 0$) is situated in the lower-left corner of the diagram. The dashed line represents well-investigated deconfinement crossover. Above this crossover, the quark-gluon matter is in the quark-gluon plasma phase, which is still a strongly correlated medium, with deconfinement and restoration of chiral symmetry. The dashed line is assumed to transform into the true phase-transition line. This line meets the axis $T = 0$ somewhere above $\mu = 300$ MeV. However, as was mentioned above, the region of finite μ is not accessible for lattice numerical simulations. The perturbative analytical calculations cannot describe the quark-gluon matter exhaustively. At the small values of μ, certain methods of calculations can be used based on lattice numerical simulations such as those based on the expansion of considered physical quantities in powers of μ. The only clear result at the right-hand side of the diagram is the line separating the phase of hadronic gas from nuclear matter. Qualitatively, transition to nuclear matter occurs when the quark chemical potential becomes larger than the constituent quark mass. In this situation quark matter becomes as dense as it is inside the atomic nuclei. Further increases of the chemical potential might lead to several phase

[*]mikhailzu@ariel.ac.il

[†]abramchuk@phystech.edu

On leave of absence from Kurchatov Complex for Theoretical and Experimental Physics of Kurchatov Institute, Bolshaya Cheremushkinskaya 25, Moscow 117259, Russia.

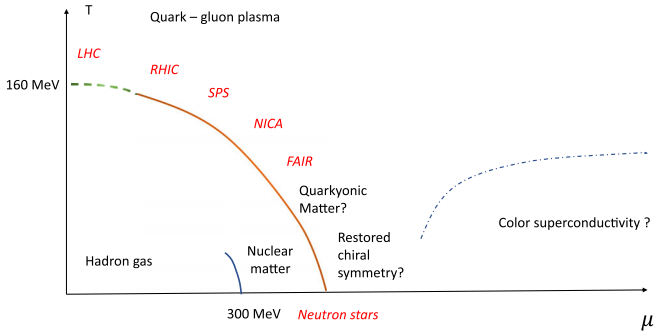

FIG. 1. We represent here the sketch of the QCD phase diagram in the plane temperature-quark chemical potential. The deconfinement crossover is represented by the dashed line. Here we have the data obtained using lattice simulations. Above the dashed line there is the quark-gluon plasma phase with restored chiral symmetry and deconfinement. At larger values of chemical potential the crossover, presumably, is changed by the true first-order phase transition. Its nature for small temperature is not yet well-established. We may actually have separate lines of the deconfinement phase transition and the chiral-symmetry restoration transition. Left to this transition (these transitions) there may be the quarkyonic phase with coexisting baryons and quarks, and the deconfining phase with restored chiral symmetry. At extremely large values of quark chemical potential several color-superconductor phases might appear. The region in the lower-left corner of the phase diagram is separated by the first order transition line to the phase of hadronic gas and nuclear matter. Modern colliders (LHC, RHIC, SPS, NICA, FAIR) will be able to probe the regions of parameters of the phase diagram along the line of the phase transition. The interior of neutron stars represent the laboratory for probe of the domain with small temperatures and large chemical potentials. According to the common lore this region is not accessible at the present moment for the existing nonperturbative QCD calculations (see, however, [26]).

transitions [25]. There are a number of hypotheses about these transitions; the corresponding part of the solid line may represent the transition to one of the phases of color superconductivity, and in addition, right to this line the so-called quarkyonic phase may be situated, where the quarks coexist with baryons. In this phase there is a confinement of quarks and the chiral symmetry is broken, as well as left to the transition line, but the sea of the particles inside the Fermi sphere consists of separate quarks. Another supposition is that the vertical transition line is to be separated into two; the confinement-deconfinement transition and the chiral-symmetry restoration line. As was mentioned above, the phenomenological methods based on perturbative QCD predict the appearance of several color superconductor phases right to the vertical transition line. The lower-right corner of the phase diagram is typically associated with the color-flavor locking color-superconductor phase.

The complementary arena for the experimental observation of nondissipative transport effects is represented by electronic quasiparticles in Dirac and Weyl semimetals [8,27–33]. These materials are used to simulate relativistic elementary particles in the laboratory. Interactions between them break emergent relativistic invariance, but even so these materials are an important way to probe elementary particle physics with strong interactions.

The chiral-separation effect (CSE) was proposed by Metlitski and Zhitnitsky [1], and it is representative of the family of nondissipative transport phenomena. This effect results in the axial current being directed along an external magnetic field in the presence of nonzero chemical potential. Originally this effect was considered in the system of continuum Dirac fermions, which would be homogeneous without an external magnetic field. In the chiral limit, i.e., for massless fermions, the axial current in these systems is proportional to the external magnetic-field strength F_{ij} and to the ordinary chemical potential μ,

$$J_5^k = \frac{1}{4\pi^2}\epsilon^{ijk0}\mu F_{ij}. \tag{1}$$

It has been proposed that this effect may be observed in the quark-gluon plasma (QGP) phase. In particular, the possibility to observe this effect experimentally during heavy-ion collisions has been discussed [2–5]. The fireballs that appeared in the noncentral collisions of heavy ions are supposed to realize the QGP phase, and are subject to strong magnetic field [6,15–24]. In the QGP phase there is no confinement of quarks, and the chiral symmetry is restored. The two colliding ions produce a strong magnetic field. After the decay of the fireball, in principle, the signature of the CSE may be found in the asymmetry of created particles. The CSE may also be relevant for the description of the quark-gluon matter at the other side of the QCD phase diagram i.e., inside the neutron stars [34]. An extension of the consideration of the CSE to the essentially nonhomogeneous systems has been performed in [35], where it has been shown that the nonhomogeneity does not affect the CSE conductivity, which remains topologically invariant and proportional to the number of the species of Dirac fermions.

Relation of the CSE to the chiral anomaly has been considered in many works [31]. The cousin of the CSE—the chiral magnetic effect (CME) [2,36–39]—has also been conjectured to be related to chiral anomaly. It has been shown, however, that in thermal equilibrium the CME is absent [11–14,40–44]. The CME is back out of equilibrium even very close to equilibrium [45]. It is also widely believed that the CME manifests itself in the steady state existing in the presence of parallel electric and magnetic fields [46]. It then may be detected through its contribution to negative magnetoresistence of Dirac semimetals [47]. At the same time the CSE exists as a true equilibrium phenomenon [9].

Using lattice regularization the CSE has been considered via analytical methods in [35,48]. This regularization also allows us to use the nonperturbative numerical

methods [14]. In [49] the results of lattice simulations for the QCD with $N_f = 2 + 1$ at finite temperature have been presented. It appears that the CSE conductivity is suppressed above the crossover temperature. Its value increases with temperature; it increases very slowly, and as we will show, it approaches the conventional expression $1/(2\pi^2)$ per Dirac fermion at the electroweak scale.

It is well-known that the theory with massless charged fermions is subject to dangerous infrared divergences [50–52]. Interaction corrections to CSE have not been considered extensively so far. In [53] it was argued that in QED high orders of perturbation theory give corrections to the CSE conductivity for the system of massive fermions. However, the calculated corrections suffer from infrared divergencies, and depend on finite photon mass, which was introduced to avoid divergences. To the best of our knowledge corrections to the CSE due to exchange by color-gauge bosons have not been considered analytically.

The present paper is devoted to the consideration of interaction corrections to the chiral separation effect. We assume, first of all, the corrections are due to strong interactions in quark matter. However, the obtained result on the topological expression for the CSE conductivity remains valid in any fermionic system with interactions, provided that the dangerous infrared divergences in the corrections to the CSE conductivity are absent. (The absence of such divergences in QCD is provided by color-magnetic confinement.) Our consideration is based on the lattice regularization of the QFT model. It remains valid, therefore, also for the consideration of the tight-binding models of solid-state systems.

As a useful tool we use Wigner-Weyl calculus in its form adopted for the lattice models. It allows us to represent the conductivities of some nondissipative transport phenomena in the form of the topological invariants. This formalism [54,55] was proposed originally as an alternative to the conventional mathematical tools of nonrelativistic quantum mechanics [56,57]. It has also been extended to be used in quantum field theory. The basic notions of this formalism are the Weyl operator symbol and the Wigner distribution function. In Wigner-Weyl calculus the quantum state is described by Wigner distribution instead of a wave function. The product of operators is replaced by the so-called star (or Moyal) product of functions in phase space.

Wigner-Weyl calculus was proposed first for the continuous systems. The attempts to construct the analogous formalism for the systems defined on a discrete lattice faced certain difficulties [58–65]. A version of lattice Wigner-Weyl calculus was proposed recently in [66]. In this version the basic properties of the Weyl operator symbols and Moyal product repeat precisely those of the continuous Wigner-Weyl calculus. In the present paper we rely on the simplified form of this calculus [67–71]. In this form the main properties of the Weyl symbols and Moyal product are not precise, and are approximate. This calculus may be used if the inhomogeneity is sufficiently weak. In solid state physics the approximate Wigner-Weyl calculus may be used when magnetic field is much smaller than 10^5 Tesla, i.e., in all realistic situations (the maximal value of magnetic field accessed in present experiments does not exceed 100 Tesla). In lattice regularized quantum field theory the approximate Wigner-Weyl calculus may be applied when the model approaches continuum limit.

We consider lattice models of a rather general type with fermions placed in the four-component Dirac spinors. For quark matter these spinors carry extra internal indices; color and flavor. In condensed matter systems the extra indices have the meaning of valley, spin, etc. The action for the fermions contains the 4×4 matrices to be expressed through Dirac matrices γ^k ($k = 1, 2, 3, 4, 5$), and their derivatives $\sigma^{kj} = \frac{i}{4}[\gamma^k, \gamma^j]$. It will always be required that at low energies the models under consideration obey chiral symmetry. This means that matrix γ^5 commutes or anticommutes with the one-particle Hamiltonian in a small vicinity of the Fermi surfaces (Fermi points). Fermi surface may be understood as the position of the singularities in momentum space for the two-point Green's function $\hat{G} = \hat{Q}^{-1}$; we will call $\hat{Q}$ the lattice Dirac operator. In the presence of weak inhomogeneity the notion of Fermi surface is to be replaced by the coordinate-dependent Fermi surface [72]. From the mathematical point of view, inhomogeneity might be considered as weak if the Wigner-transformed Green's function $G_W(p, x)$ has singularities for any value of x very close to the positions of the zeros of the Weyl symbol $Q_W(p, x)$ of operator $\hat{Q}$. This will give the definition of the Fermi surface in the case of weak inhomogeneity.

In [35] it has been shown that if low-energy effective theory obeys chiral symmetry, the axial current of CSE in the nonhomogeneous system of the general type is still proportional to an external magnetic field. Averaged over the whole volume of the system its response to the chemical potential may be expressed as

$$\frac{d}{d\mu}\bar{J}^k_5 = \frac{\mathcal{N}}{4\pi^2}\epsilon^{ijk0}F_{ij}, \tag{2}$$

where $\mathcal{N}$ is a topological invariant expressed through G_W and Q_W,

$$\mathcal{N} = \frac{1}{48\pi^2\mathbf{V}}\int_{\Sigma_3}\int d^3x\,\mathrm{tr}[\gamma^5 G_W \star dQ_W \star G_W \wedge \star dQ_W \star G_W \star \wedge dQ_W], \tag{3}$$

where Q_W and G_W are defined for the system without an external magnetic field. The above expression has been derived for the noninteracting system. The surface Σ_3 in momentum space in the general case depends on x. It surrounds the singularities of an expression standing inside

the integral. $\mathcal{N}$ is robust to smooth modification of the system if this modification does not break chiral symmetry around Σ_3. For sufficiently weak homogeneity the value of $\mathcal{N}$ may be calculated easily, and is given by the number of the species of chiral Dirac fermions in the low-energy effective theory. As a result the CSE conductivity is given by $N_c N_f/(2\pi^2)$ for the system of N_f noninteracting quarks ($N_c = 3$ is the number of colors).

In the present paper we prove that Eqs. (2) and (3) remain valid in the interacting system, when the Green's function G is replaced by the complete-interacting renormalized Green's function. Correspondingly, $\hat{Q}$ is defined as its inverse. In QCD this may be applied directly to the region of the phase diagram with small temperatures and large values of μ if at those values of μ the chiral symmetry is restored, while gap is not opened, i.e., there is no color superconductivity. Besides, the same result may be applied to the electronic quasiparticles in Weyl semimetals, which simulate high-energy physics in the laboratory. Here we need $\mu \gg T$.

In QCD at finite temperature Eqs. (2) and (3) may be applied to the quark-gluon plasma phase provided that the temperature may be neglected compared to the quark chemical potential. In advance, it is not clear to which degree μ has to be larger than T in order to apply the topological expression. In order to clarify this we calculate the nonperturbative contributions to the CSE conductivity using the method of field correlators developed by Yu. A. Simonov and collaborators [25,26,73–80]. At the values of μ and T around T_c the $SU(3)$ coupling constant is $\alpha_s(T_c) \approx 0.3$, and the perturbative corrections are expected to contribute by amount of about 30%. We disregard these contributions completely. Therefore, we assume that the qualitative estimate is only in the region $T \sim \mu \sim T_c$. However, at larger values of T and/or μ, α_s decreases; at the energy scale of order of 1 GeV it becomes of order 0.2, then the perturbative corrections become smaller. The obtained results demonstrate that in the phase diagram (see Fig. 1) the topological result remains far from the region accessible by modern colliders. For example, in the region of the phase diagram, where RHIC operates, the CSE conductivity is suppressed by a factor ~ 2 compared to the conventional value.

II. WIGNER-WEYL FORMALISM IN LATTICE THEORY IN THE PRESENCE OF INTERACTIONS

A. Partition function of noninteracting system

First we consider the noninteracting fermion system in lattice regularization. We refer here to the system of quarks. However, the obtained results do not depend on the nature of the fermions, and they remain valid for any fermionic system with chiral fermions.

In Euclidian spacetime the partition function is expressed through the inverse bare Green function. It will be called further the Dirac operator and denoted by $\hat{Q}$. The partition function is given by

$$Z = \int D\bar{\psi} D\psi \, e^{S[\psi,\bar{\psi}]}. \tag{4}$$

Here $\psi, \bar{\psi}$ are the Grassmann-valued quark fields, while S is the action

$$\begin{aligned} S[\psi,\bar{\psi}] &= \int_{\mathcal{M}} \frac{d^D p}{|\mathcal{M}|} \bar{\psi}(p) \hat{Q}(i\partial_p, p) \psi(p) \\ &= \int_{\mathcal{M}} \frac{d^D p}{|\mathcal{M}|} \bar{\psi}^a(p) \hat{Q}^{ab}(i\partial_p, p) \psi^b(p) \\ &= \sum_{r_n} \int_{\mathcal{M}} \frac{d^D p}{|\mathcal{M}|} Q_W^{ab}(r_n, p) W^{ba}(r_n, p) \\ &= \sum_{r_n} \int_{\mathcal{M}} \frac{d^D p}{|\mathcal{M}|} \mathrm{tr}[Q_W(r_n, p) W(r_n, p)], \end{aligned} \tag{5}$$

where we used Weyl symbols of operators

$$Q_W(x, p) \equiv \int_{\mathcal{M}} dq e^{ixq} \langle p + q/2 | \hat{Q} | p - q/2 \rangle, \tag{6}$$

and

$$W(r_n, p) = (|\psi\rangle\langle\psi|)_W. \tag{7}$$

Here by $|\psi\rangle\langle\psi|$ we denote operator with Grassmann—valued matrix elements $\psi(x)\bar{\psi}(y)$. For simplicity of notations we discretize both space coordinates and imaginary time. In the case of the condensed-matter system we are able to take off the discretization of imaginary time in order to arrive at the conventional expression $\hat{Q} = i\omega - \hat{H}$, where $\hat{H}$ is the one-particle Hamiltonian.

Using *Peierls* substitution in the presence of a slowly-varying gauge field Eq. (6) takes the form

$$Q_W(r, p) \to Q_W(r, p - A(r)). \tag{8}$$

Here direct dependence on r is caused by the other slow-varying external fields. The partition function receives the form

$$Z = \int D\bar{\psi} D\psi \exp\left(-\sum_{r_n} \int_{\mathcal{M}|} \frac{d^D p}{|\mathcal{M}|} \mathrm{tr}[Q_W(r_n, p) W(r_n, p)] \right). \tag{9}$$

The propagator of fermions is defined as

$$\begin{aligned} \hat{G} = -\frac{1}{Z} \int D\bar{\psi} D\psi |\psi\rangle\langle\bar{\psi}| \\ \times \exp\left(\int \frac{d^D p}{|\mathcal{M}|} \bar{\psi}(p) \hat{Q}(i\partial_p, p) \psi(p) \right), \end{aligned} \tag{10}$$

and its expression in momentum space is

$$G(p_1,p_2)=\langle p_1|G|p_2\rangle = \frac{1}{Z}\int D\bar\psi D\psi\bar\psi(p_2)\psi(p_1)\exp\left(\int\frac{d^Dp}{|\mathcal{M}|}\bar\psi(p)\hat Q(i\partial_p,p)\psi(p)\right). \tag{11}$$

B. Partition function for the system with interactions

Let us consider the case of interactions between the fermions. As above we speak first of all of the systems, in which the fermions are quarks, while the gauge group is the color $SU(3)$ of strong interactions. However, the expressions to be derived further are valid also for the other interactions, and the other fermions with chiral symmetry. This brings the partition function to the form

$$Z=\int D\bar\psi D\psi DAe^{-S_A[A]}\exp\left(-\sum_{r_n}\int_{\mathcal{M}|}\frac{d^Dp}{|\mathcal{M}|}\mathrm{tr}[Q_W(r_n,p-A)W(r_n,p)]\right). \tag{12}$$

Here A is $SU(3)$ gauge field, while $S_A[A]$ is the pure gauge field action, which contains the gauge fixing term [we are speaking here of the gauge group $SU(3)$ only].

A variation of the partition function may be expressed as follows:

$$\begin{aligned}\delta\log Z&=-\frac{1}{Z}\int D\bar\psi D\psi DAe^{-S_A[A]}\left[\sum_{r_n}\int\frac{d^Dq}{|\mathcal{M}|}\delta Q_W^{ab}(r_n,q-A)W^{ba}(r_n,q)\right]\exp\left(-\sum_{r_n}\int\frac{d^Dp}{|\mathcal{M}|}Q_W^{ab}(r_n,p-A)W^{ba}(r_n,p)\right)\\&=-\sum_{r_n}\int DAe^{-S_A[A]}\frac{d^Dq}{|\mathcal{M}|}\delta Q_W^{ab}(r_n,q-A)\left[\frac{1}{Z}\int D\bar\psi D\psi W^{ba}(r_n,q-A)\exp\left(-\sum_{r_n}\int\frac{d^Dp}{|\mathcal{M}|}Q_W^{ab}(r_n,p-A)W^{ba}(r_n,p)\right)\right]\\&=\sum_{r_n}\int DAe^{-S_A[A]}\frac{d^Dq}{|\mathcal{M}|}\delta Q_W^{ab}(r_n,q-A)G_W^{ba}(r_n,q-A)\\&=\sum_{r_n}\int DAe^{-S_A[A]}\frac{d^Dq}{|\mathcal{M}|}\mathrm{tr}[\delta Q_W(r_n,q-A)G_W(r_n,q-A)].\end{aligned}$$

In the case when dependence of $\delta Q_W(r_n,q-A)$ on A may be neglected, we obtain

$$\begin{aligned}\delta\log Z&=\sum_{r_n}\int\frac{d^Dp}{|\mathcal{M}|}\mathrm{tr}[\delta Q_W(r_n,p)\mathbf{G}_W(r_n,p)]\\&=\int d^Dx\int\frac{d^Dp}{\mathbf{v}|\mathcal{M}|}\mathrm{tr}[\delta Q_W(x,p)\mathbf{G}_W(x,p)]\\&=\int d^Dx\int\frac{d^Dp}{(2\pi)^D}\mathrm{tr}[\delta Q_W(x,p)\mathbf{G}_W(x,p)].\end{aligned} \tag{13}$$

Here $\mathbf{v}$ is the elementary lattice-cell volume. In the second line assume that the expression standing under the sum depends slowly on r_n. In the last line we use that $\mathbf{v}|\mathcal{M}|=(2\pi)^D$. We rewrite this expression as

$$\delta\log Z=\mathrm{tr}[\hat{\mathbf{G}}\delta\hat Q]=\mathrm{Tr}[\mathbf{G}_W\star\delta Q_W]=\mathrm{Tr}[\mathbf{G}_W\delta Q_W] \tag{14}$$

with

$$\star=e^{\frac{i}{2}(\overleftarrow{\partial}_x\overrightarrow{\partial}_p-\overleftarrow{\partial}_p\overrightarrow{\partial}_x)}.$$

Here by G we denote the complete interacting two-point quark Green's function while G is the Green's function in the presence of an external $SU(3)$ field A. Notice that $\mathbf{G}$ is the quark Green's function calculated in certain gauge of the $SU(3)$ group. Our further results do not depend on the particular choice of the gauge. The star may be removed here if $\delta Q_W(p,x)$ as a function of x is localized in a finite region of space. In the following we will always denote the complete Green function and its inverse by bold letters, while ordinary letters will denote bare quantities with no interactions taken into account.

From now on we use continuum limit for the coordinates $r_n\to x$. This is possible if variations of fields on the distances of the order of lattice spacings are neglected.

In the presence of an extra external gauge field we substitute $p\to p-\mathcal{A}$

$$Q_W(x,p-A)\to Q_W(x,p-A-\mathcal{A}). \tag{15}$$

Variation with respect to the external gauge field $\mathcal{A} \to \mathcal{A} + \delta\mathcal{A}$ gives

$$Q_W(x, p - A - (\mathcal{A} + \delta\mathcal{A})) = Q_W(x, p - A - \mathcal{A}) + \partial_{\mathcal{A}_i} Q_W(x, p - A - \mathcal{A})\delta\mathcal{A}_i \quad (16)$$

and

$$\delta Q_W = \partial_{\mathcal{A}_i} Q_W \delta\mathcal{A}_i = -\partial_{p_i} Q_W \delta\mathcal{A}_i. \quad (17)$$

The expression for $\partial_{p_i} Q_W(x, p - A)$ obviously becomes independent of A, when we approach the continuum limit. Since we are interested in continuum limit of lattice theory, the electric current may be taken in the form

$$j_i(x) = \frac{\delta \log Z}{\delta \mathcal{A}_k(x)} = -\int_{(2\pi)^D} \frac{d^D p}{|\mathcal{M}|} \mathrm{tr}[\mathbf{G}_W(x, p)\partial_{p_i} Q_W(x, p)]. \quad (18)$$

Based on analogy with electric current the naive expression for local axial current density may be defined as

$$j^5_k(x) = -\int_{\mathcal{M}} \frac{d^D p}{(2\pi)^D} \mathrm{tr}[\gamma^5 \mathbf{G}_W(x, p)\partial_{p_k} Q_W(x, p)]. \quad (19)$$

C. Gauge transformation of Weyl symbol

The $U(1)$ gauge transformation acts as $|x\rangle \to e^{i\alpha(x)}|x\rangle$. As a result the Weyl symbol of an operator $\hat{B}$ is transformed as

$$B_W(x, p) = \int dy e^{-iyp} \langle x + y/2|\hat{B}|x - y/2\rangle \to \int dy e^{-iyp + i\alpha(x+y/2) - i\alpha(x-y/2)} \times \langle x + y/2|\hat{B}|x - y/2\rangle. \quad (20)$$

Here we replace the sum over lattice points by an integral because we assume that all fields vary slowly, so that their variation at the distance of lattice spacing may be neglected. Let us consider those gauge transformations for which the function α almost does not vary at the distances of the order of the correlation-length λ characterizing operator $\hat{B}$, i.e., $|\lambda\partial\alpha| \ll 1$. We call these transformations "slow" (with respect to $\hat{B}$). For them we obtain:

$$B_W(x, p) \to \int dy e^{-iyp + i\alpha(x+y/2) - i\alpha(x-y/2)} \times \langle x + y/2|\hat{B}|x - y/2\rangle \approx \int dy e^{-iy(p - \partial\alpha(x))} \langle x + y/2|\hat{B}|x - y/2\rangle = B_W(x, p - \partial\alpha(x)). \quad (21)$$

If operator $\hat{B}$ depends on the $U(1)$ gauge field A then we may require that the gauge transformation of $\hat{B}$ should be compensated by the gauge transformation of field A. This occurs, for example, for Dirac operator $\hat{Q}$ due to gauge invariance of the whole model. Consideration of "slow" gauge transformation results in the requirement that Weyl symbol $B_W(x, p)$ depends on $A(x)$ through the functional dependence on $p - A(x)$, and gauge-invariant quantities; field strength F_{ij} and its derivatives, provided that variation of $A(x)$ may be neglected at the distances of the order of λ, i.e., $|\lambda^2 F_{ij}| \ll 1$. As a result for such $A(x)$ we may represent B_W as a series

$$B_W(x, p) = B^{(0)}_W(x, p - A(x)) + B^{(1)}_{(ij)W}(x, p - A(x))F_{ij}(x) + B^{(2)}_{(ijk)W}(x, p - A(x))\partial_k F_{ij}(x) + \cdots. \quad (22)$$

Here dots denote the higher-order terms in derivatives. This expansion is reasonable, i.e., the higher-order terms are smaller than the lower-order terms under the same condition $|\lambda^2 F_{ij}| \ll 1$.

In particular, for bare $\hat{Q}$ the correlation length λ is given by the lattice spacing, and we arrive at Eq. (8) for the fields A that vary slowly at the distance of the order of lattice spacing.

D. Renormalized quark velocity and renormalized axial current

The meaning of $-\partial_{p_i} Q_W(x, p - A)$ is matrix of bare quark velocity. It is natural that the electric current is (up to electric charge of quark) given by averaging of quark velocity. A natural supposition is that in quantum theory the renormalized quark velocity has to be substituted to this expression. Namely, let us denote by $\mathbf{Q}$ an operator inverse to $\mathbf{G}$, which is the complete quark Green's function with interactions taken into account. Notice again that both $\mathbf{G}$ and $\mathbf{Q}$ are to be calculated after the gauge-fixing procedure for $SU(3)$ gauge group. Then the renormalized velocity operator is

$$v_R = -\partial_{p_i} \mathbf{Q}_W(x, p - A). \quad (23)$$

It can be shown using the methodology developed in [81] that to all orders in perturbation theory the electric current averaged over the system volume V is given by

$$\frac{1}{\beta V}\int d^D x j_k(x) = -\frac{1}{\beta V}\int_{\mathcal{M}} d^D x \frac{d^D p}{(2\pi)^D} \times \mathrm{tr}[\mathbf{G}_W(x,p)\partial_{p_i}\mathbf{Q}_W(x,p)].$$

The latter expression does not have much sense because according to the Bloch theorem the persistent current vanishes in nonmarginal systems. The proof of the theorem follows from the fact that the above expression is a topological invariant. At the same time the above expression does not mean that the local current density may be expressed through the renormalized velocity operator

$$j_k(x) \neq -\int_{\mathcal{M}} \frac{d^D p}{(2\pi)^D}\mathrm{tr}[\mathbf{G}_W(x,p)\partial_{p_i}\mathbf{Q}_W(x,p)].$$

The nontrivial expression appears, however, when we consider response of the above expression to external fields. In this way considering the electric field that has equal values but opposite directions in the two pieces of space, in [81] it has been shown that the (integer) Hall conductivity (averaged over the system area) does not have perturbative corrections, and may be expressed through the complete interacting Green functions. As a result, we can take the "renormalized" expression for the electric current density

$$\mathbf{j}_k(x) = -\int_{\mathcal{M}} \frac{d^D p}{(2\pi)^D}\mathrm{tr}[\mathbf{G}_W(x,p)\partial_{p_i}\mathbf{Q}_W(x,p)]$$

and calculate its response to electric field. This way the correct expression for the Hall conductance is reproduced, while the longitudinal contribution vanishes. We conclude that for the calculation of the physical observables averaged over the whole system area in the Quantum Hall Effect (QHE) systems the renormalized expression for the current density may be used.

Based on an analogy to electric conductivity below we accept as the definition of the renormalized axial current the expression with the operator of renormalized velocity in place of the bare velocity,

$$\mathbf{j}^5_k(x) = -\int_{\mathcal{M}} \frac{d^D p}{(2\pi)^D}\mathrm{tr}[\gamma^5\mathbf{G}_W(x,p)\partial_{p_k}\mathbf{Q}_W(x,p)]. \quad (24)$$

For the calculation of the electric current the QHE system integral over the whole Brillouin zone is to be calculated. We will see that contrary to this for the calculation of CSE conductivity one should integrate in momentum space along the infinitely small hypersurface surrounding the position of Fermi surface/Fermi point. As a result in the field theory with spatial isotropy at zero temperature and zero chemical potential (for example, in QED) we need expression for $\partial_{p_k}\mathbf{Q}_W(x,p)$ in the small vicinity of $p=0$. There, we have

$$\partial_{p_k}\mathbf{Q}_W(x,p) \approx \gamma^k Z_F.$$

Here Z_F is the fermion field renormalization constant. One can see, therefore, that at $T=\mu=0$ the only difference if we substitute to the CSE current the renormalized velocity (instead of the bare one) is appearance of the renormalization constant Z_F. However, this is precisely what is to be done for the calculation of the renormalized axial current at $T=\mu=0$ (if the latter is defined as $\langle\bar{\Psi}_R\gamma^\mu\gamma^5\Psi_R\rangle$, where $\Psi_R = Z_F^{1/2}\Psi$ is the renormalized field operator, while Ψ is bare fermionic field). Notice, that unlike vector current the axial current is not Noether current responsible for the transport of a conserved charge. Therefore, its definition in the interacting systems is flexible. In the present paper we extend definition of Eq. (24) to the systems with nonzero T and μ, and to the systems with spatial anisotropy. As it was mentioned above, Eq. (24) will be considered below as the definition of renormalized axial current.

E. Groenewold equation and its iterative solution

The (renormalized) Dirac operator and (renormalized) Green's function obey the following equation

$$\hat{\mathbf{Q}}\,\hat{\mathbf{G}} = 1. \quad (25)$$

A Weyl-Wigner transformation results in the Groenewold equation

$$\mathbf{Q}_W(p,x)\star\mathbf{G}_W(p,x) = 1. \quad (26)$$

We assume here that all external fields vary slowly, i.e., these variations may be neglected at the distance of the order of lattice spacing. Then Weyl symbol of bare (noninteracting) Dirac operator has the functional dependence $Q_W(p-A(x),x)$ in the presence of external field $A_i(x)$ (corresponding to the field strength F_{ij}). Here the coordinate dependence caused by the other external fields is given by direct dependence on x. The function $\mathbf{Q}_W(p,x)$ with interaction corrections can be represented as

$$\mathbf{Q}_W(p,x) = \mathbf{Q}^{(0)}_W(p-A(x),x) + \mathbf{Q}^{(1)}_{(ij)W}(p-A(x),x)F_{ij} + \cdots. \quad (27)$$

Dots represent the terms proportional to the higher powers of F and the derivatives of F. As was explained above in Sec. II C, this expansion is valid under the condition $|\lambda^2 F_{ij}| \ll 1$, where λ is the correlation length associated with the given interacting system. This expansion is reasonable, at least when we consider the DC CSE conductivity, i.e., the response of the axial current to sufficiently small external magnetic field. Recall that the correlation length associated with the bare Dirac operator is

equal to the lattice spacing. In the presence of interactions the correlation length may become much larger, of the order of the existing dimensional parameters of the system. For example, for the quark matter at zero temperature such parameters are the quark chemical potential and $\Lambda_{\rm QCD}$. Assuming $\mu > \Lambda_{\rm QCD}$, for these systems Eq. (27) may be applied for magnetic fields much smaller than $\Lambda^2_{\rm QCD}$.

In order to illustrate a representation of Eq. (27) let us consider the approximation when only the one-gluon exchange is taken into account,

$$\mathbf{Q}^{(0)}_W(p-A(x),x) \approx Q_W(p-A(x),x) - g^2 \int \frac{d^D k}{(2\pi)^D} \mathcal{D}^{(0)ab}_{\mu\nu}(k)\gamma^\mu t_a G^{(0)}_W(p-k-A(x),x)\gamma^\nu t_b,$$
$$\mathbf{Q}^{(1)}_{(ij)W}(p-A(x),x) \approx -g^2 \int \frac{d^D k}{(2\pi)^D} \mathcal{D}^{(0)ab}_{\mu\nu}(k)\gamma^\mu t_a G^{(1)}_{(ij)W}(p-k-A(x),x)\gamma^\nu t_b. \quad (28)$$

Here $\mathcal{D}^{(0)}$ is the gluon propagator, while t_a are the Gell-Mann matrices, and a, b are the color indices. Above we denote by $G^{(0)}_W(p,x)$ solution of reduced Groenewold equation [i.e., the one without $A(x)$],

$$G^{(0)}_W(p,x)\star Q_W(p,x) = 1.$$

At the same time the first-order term in derivative of A is

$$G^{(1)}_{(ij)W} = \frac{i}{2}[G^{(0)}_W \star (\partial_{p_i} Q^{(0)}_W)\star G^{(0)}_W \star (\partial_{p_j} Q^{(0)}_W)\star G^{(0)}_W].$$

It gives the first-order term (expansion over derivatives of A) in solution of equation

$$(G^{(0)}_W(p,x) + G^{(1)}_{(ij)W}F_{ij})\star Q_W(p-A(x),x) = 1.$$

This result follows the derivation presented in [82] and is based on the expansion

$$\star = 1 + \frac{i}{2}(\overleftarrow{\partial}_x\overrightarrow{\partial}_p - \overleftarrow{\partial}_p\overrightarrow{\partial}_x) + \cdots.$$

Among the second-order diagrams let us consider the representative one, in which the gluon propagator receives correction from the quark loop. This gives the following contribution to quark self-energy up to the linear terms in F_{ij}:

$$\Delta\Sigma = g^2 \int \frac{d^D k}{(2\pi)^D} \mathcal{D}^{(1)ab}_{\mu\nu W}(k,x)\gamma^\mu t_a G^{(0)}_W(p-k-A(x),x)\gamma^\nu t_b + g^2 \int \frac{d^D k}{(2\pi)^D} F_{ij}\mathcal{D}^{(0)ab}_{\mu\nu W}(k,x)\gamma^\mu t_a G^{(1)}_{(ij)W}(p-k-A(x),x)\gamma^\nu t_b,$$

where $-\Delta\Sigma$ is one of the many terms entering perturbative expansion of $\mathbf{Q}_W(p,x)$. The corresponding contribution to gluon propagator is

$$\begin{aligned}
\mathcal{D}^{(1)ab}_{\mu\nu W}(k,x) &= g^2 \mathcal{D}^{(0)ac}_{\mu\rho W}(k)\star \int \frac{d^D q}{(2\pi)^D} \mathrm{tr}(G_W(-q,x)\gamma^\rho t^b G_W(k-q,x)\gamma^\sigma t^d)\star \mathcal{D}^{(0)db}_{\sigma\nu W}(k) \\
&= g^2 \mathcal{D}^{(0)ac}_{\mu\rho W}(k)\star \int \frac{d^D q}{(2\pi)^D} \mathrm{tr}(G^{(0)}_W(-q+A(x),x)\gamma^\rho t^b G^{(0)}_W(k-q-A(x),x)\gamma^\sigma t^d)\star \mathcal{D}^{(0)db}_{\sigma\nu W}(k) \\
&\quad + g^2 \mathcal{D}^{(0)ac}_{\mu\rho W}(k)\star \int \frac{d^D q}{(2\pi)^D} \mathrm{tr}(G^{(0)}_W(-q+A(x),x)\gamma^\rho t^b G^{(1)}_{(ij)W}(k-q-A(x),x)\gamma^\sigma t^d)\star \mathcal{D}^{(0)db}_{\sigma\nu W}(k)F_{ij} \\
&\quad - g^2 \mathcal{D}^{(0)ac}_{\mu\rho W}(k)\star \int \frac{d^D q}{(2\pi)^D} \mathrm{tr}(G^{(1)}_{(ij)W}(-q+A(x),x)\gamma^\rho t^b G^{(0)}_W(k-q-A(x),x)\gamma^\sigma t^d)\star \mathcal{D}^{(0)db}_{\sigma\nu W}(k)F_{ij} \\
&= g^2 \mathcal{D}^{(0)ac}_{\mu\rho W}(k)\star \int \frac{d^D q}{(2\pi)^D} \mathrm{tr}(G^{(0)}_W(-q,x)\gamma^\rho t^b G^{(0)}_W(k-q,x)\gamma^\sigma t^d)\star \mathcal{D}^{(0)db}_{\sigma\nu W}(k) \\
&\quad + g^2 \mathcal{D}^{(0)ac}_{\mu\rho W}(k)\star \int \frac{d^D q}{(2\pi)^D} \mathrm{tr}(G^{(0)}_W(-q,x)\gamma^\rho t^b G^{(1)}_{(ij)W}(k-q,x)\gamma^\sigma t^d)\star \mathcal{D}^{(0)db}_{\sigma\nu W}(k)F_{ij} \\
&\quad - g^2 \mathcal{D}^{(0)ac}_{\mu\rho W}(k)\star \int \frac{d^D q}{(2\pi)^D} \mathrm{tr}(G^{(1)}_{(ij)W}(-q,x)\gamma^\rho t^b G^{(0)}_W(k-q,x)\gamma^\sigma t^d)\star \mathcal{D}^{(0)db}_{\sigma\nu W}(k)F_{ij}. \quad (29)
\end{aligned}$$

In the last three rows we performed the shift of variable $q - A(x) \to q$. One can see that still there are the two types of the contributions to $\mathbf{Q}_W(p,x)$ described by Eq. (27). Obviously the same consideration may be extended to all orders of

perturbation theory. The same refers also to the nonperturbative contributions to $\mathbf{Q}_W(p,x)$ according to the arguments presented in Sec. II C.

In the similar way the solution of Groenewold equation (26) for the interacting Green function (up to the linear terms in F) is given by

$$\mathbf{G}_W(p,x) \approx \mathbf{G}_W^{(0)}(p,x) + \mathbf{G}_{(ij)W}^{(1)} F_{ij},$$

where $\mathbf{G}_W^{(0)}(p,x)$ is solution of reduced Groenewold equation [i.e., the one without $A(x)$],

$$\mathbf{G}_W^{(0)}(p,x) \star \mathbf{Q}_W^{(0)}(p,x) = 1.$$

The first-order term in derivative of A is more complicated than in the case of the noninteracting Green function,

$$\mathbf{G}_{(ij)W}^{(1)} = \frac{i}{2}\left[\mathbf{G}_W^{(0)} \star (\partial_{p_i}\mathbf{Q}_W^{(0)}) \star \mathbf{G}_W^{(0)} \star (\partial_{p_j}\mathbf{Q}_W^{(0)}) \star \mathbf{G}_W^{(0)}\right] F_{ij} - \mathbf{G}_W^{(0)} \star \mathbf{Q}_{(ij)W}^{(1)} \star \mathbf{G}_W^{(0)} F_{ij}. \tag{30}$$

III. TOPOLOGICAL EXPRESSION FOR CHIRAL SEPARATION EFFECT IN THE PRESENCE OF INTERACTIONS AT $T = 0$

A. Response of axial current to magnetic field

As has been explained above, the local (renormalized) axial current density is given by

$$\mathbf{j}_k^5(x) = -\int_{\mathcal{M}} \frac{d^D p}{(2\pi)^D} \mathrm{tr}[\gamma^5 \mathbf{G}_W(x,p) \partial_{p_k} \mathbf{Q}_W(x,p)]. \tag{31}$$

We obtain the following term with the linear response to external field strength,

$$\begin{aligned}\mathbf{j}_k^5(x) = &-\frac{i}{2}\int_{\mathcal{M}} \frac{d^D p}{(2\pi)^D} \mathrm{tr}\Big[\gamma^5 \Big[\mathbf{G}_W^{(0)} \star (\partial_{p_i}\mathbf{Q}_W^{(0)}) \star \mathbf{G}_W^{(0)} \star (\partial_{p_j}\mathbf{Q}_W^{(0)}) \star \mathbf{G}_W^{(0)}\Big] \partial_{p_k}\mathbf{Q}_W^{(0)}\Big] F_{ij} \\ &+ \int_{\mathcal{M}} \frac{d^D p}{(2\pi)^D} \mathrm{tr}\Big[\gamma^5 \Big[\mathbf{G}_W^{(0)} \star \mathbf{Q}_{(ij)W}^{(1)} \star \mathbf{G}_W^{(0)}\Big] \partial_{p_k}\mathbf{Q}_W^{(0)}\Big] F_{ij} \\ &- \int_{\mathcal{M}} \frac{d^D p}{(2\pi)^D} \mathrm{tr}\Big[\gamma^5 \mathbf{G}_W^{(0)} \partial_{p_k}\Big[\mathbf{Q}_{(ij)W}^{(1)}\Big]\Big] F_{ij}.\end{aligned} \tag{32}$$

Averaging the local current over the whole system volume we get

$$\begin{aligned}\bar{J}_i^5 &\equiv \frac{1}{\beta \mathbf{V}} \sum_x \mathbf{j}_i^5(x) \\ &= -\frac{1}{\beta \mathbf{V}} \int d^D x \int_{\mathcal{M}} \frac{d^D p}{\mathbf{v}|\mathcal{M}|} \mathrm{tr}[\gamma^5 \mathbf{G}_W(x,p) \partial_{p_i} \mathbf{Q}_W(x,p)] \\ &= -\frac{1}{\beta \mathbf{V}} \mathrm{Tr}[\gamma^5 \mathbf{G}_W(x,p) \partial_{p_i} \mathbf{Q}_W(x,p)].\end{aligned} \tag{33}$$

Here $\mathbf{v}$ is volume of the lattice cell. We have a useful formula $\mathbf{v}|\mathcal{M}| = (2\pi)^D$ and we obtain

$$\begin{aligned}\bar{J}_k^5 = -\frac{i}{2}\frac{1}{\beta \mathbf{V}} \int d^D x \int_{\mathcal{M}} \frac{d^D p}{(2\pi)^D} \mathrm{tr}\Big[\gamma^5 \Big[&\mathbf{G}_W^{(0)} \star (\partial_{p_i}\mathbf{Q}_W^{(0)}) \\ &\star \mathbf{G}_W^{(0)} \star (\partial_{p_j}\mathbf{Q}_W^{(0)}) \star \mathbf{G}_W^{(0)} \partial_{p_k}\mathbf{Q}_W^{(0)} \\ &+ 2i\mathbf{G}_W^{(0)} \star \mathbf{Q}_{(ij)W}^{(1)} \star \mathbf{G}_W^{(0)} \partial_{p_k}\mathbf{Q}_W^{(0)} - 2i\mathbf{G}_W^{(0)} \partial_{p_k}\Big[\mathbf{Q}_{(ij)W}^{(1)}\Big]\Big]\Big] F_{ij}.\end{aligned} \tag{34}$$

B. Axial current for massless fermions at finite temperature

For the sake of regularization and also because we are going to consider QCD at finite temperature, we introduce finite temperature. Matsubara frequencies are $p_4 = \omega_n = \frac{2\pi(n+\frac{1}{2})}{\beta}$. Here the inverse temperature $\beta = 1/T$ is taken in lattice units; $N_t \equiv \frac{1}{T}$, the values of p_4 are $p_4 = \frac{2\pi(n_4+\frac{1}{2})}{N_t}$, and $n_4 = -\frac{N_t}{2}, \ldots, \frac{N_t}{2} - 1$. The boundary values are $\omega_{n=-\frac{N_t}{2}} = \frac{2\pi(-\frac{N_t}{2}+\frac{1}{2})}{N_t} = -\pi + \frac{\pi}{N_t}$ and $\omega_{n=\frac{N_t}{2}-1} = \frac{2\pi(\frac{N_t}{2}-\frac{1}{2})}{N_t} = \pi - \frac{\pi}{N_t}$. The Matsubara frequencies closest to zero are $\omega_{n=0} = \frac{\pi}{N_t}$ and $\omega_{n=-1} = -\frac{\pi}{N_t}$. One can see that ω_n never equals to zero. Therefore, the propagator does not have poles in momentum space. The axial current receives the form

$$\begin{aligned}\bar{J}_k^5 = -\frac{i}{2}\frac{1}{\beta \mathbf{V}} \sum_{n=-\frac{N_t}{2}}^{\frac{N_t}{2}-1} \int d^3 x \int_{\mathcal{M}_3} \frac{d^3 p}{(2\pi)^3} \\ \times \mathrm{tr}\Big[\gamma^5 \Big[&\mathbf{G}_W^{(0)} \star (\partial_{p_i}\mathbf{Q}_W^{(0)}) \star \mathbf{G}_W^{(0)} \star (\partial_{p_j}\mathbf{Q}_W^{(0)}) \star \mathbf{G}_W^{(0)} \partial_{p_k}\mathbf{Q}_W^{(0)} \\ &+ 2i\mathbf{G}_W^{(0)} \star \mathbf{Q}_{(ij)W}^{(1)} \star \mathbf{G}_W^{(0)} \partial_{p_k}\mathbf{Q}_W^{(0)} - 2i\mathbf{G}_W^{(0)} \partial_{p_k}\Big[\mathbf{Q}_{(ij)W}^{(1)}\Big]\Big]\Big] F_{ij}.\end{aligned} \tag{35}$$

Chemical potential may be introduced as $\omega_n \to \omega_n - i\mu$. Therefore, the response of axial current to variation of chemical potential $\delta\mu$ and to external field strength $F_{\mu\nu}$ receives the form

$$\begin{aligned}\bar{J}_k^5 = -\frac{1}{2\mathbf{V}\beta} \sum_{n=-\frac{N_t}{2}}^{\frac{N_t}{2}-1} \int d^3 x \int_{\mathcal{M}_3} \frac{d^3 p}{(2\pi)^3} \partial_{\omega_n} \mathrm{tr}\Big[\gamma^5 \Big[&\mathbf{G}_W^{(0)} \star (\partial_{p_i}\mathbf{Q}_W^{(0)}) \star \mathbf{G}_W^{(0)} \star (\partial_{p_j}\mathbf{Q}_W^{(0)}) \star \mathbf{G}_W^{(0)} \partial_{p_k}\mathbf{Q}_W^{(0)} \\ &+ 2i\mathbf{G}_W^{(0)} \star \mathbf{Q}_{(ij)W}^{(1)} \star \mathbf{G}_W^{(0)} \partial_{p_k}\mathbf{Q}_W^{(0)} - 2i\mathbf{G}_W^{(0)} \partial_{p_k}\Big[\mathbf{Q}_{(ij)W}^{(1)}\Big]\Big]\Big] F_{ij}\delta\mu.\end{aligned} \tag{36}$$

We represent the above expression as

$$\bar{J}^5_k(x) = \sigma_{ijk} F_{ij} \delta\mu, \tag{37}$$

where

$$\sigma_{ijk} = -\frac{1}{2\mathbf{V}\beta} \sum_{n=-\frac{N_t}{2}}^{\frac{N_t}{2}-1} \int d^3x \int_{\mathcal{M}_3} \frac{d^3p}{(2\pi)^3} \partial_{\omega_n} \mathrm{tr}\Big[\gamma^5 \Big[\mathbf{G}^{(0)}_W \star (\partial_{p_i} \mathbf{Q}^{(0)}_W) \star \mathbf{G}^{(0)}_W \star (\partial_{p_j} \mathbf{Q}^{(0)}_W) \star \mathbf{G}^{(0)}_W \partial_{p_k} \mathbf{Q}^{(0)}_W + 2i \mathbf{G}^{(0)}_W \star \mathbf{Q}^{(1)}_{(ij)W} \star \mathbf{G}^{(0)}_W \partial_{p_k} \mathbf{Q}^{(0)}_W - 2i \mathbf{G}^{(0)}_W \partial_{p_k} \Big[\mathbf{Q}^{(1)}_{(ij)W}\Big]\Big]\Big] \tag{38}$$

has the meaning of the CSE conductivity when the external field strength corresponds to a constant magnetic field H: $F_{ij} = -\epsilon_{ijk} H_k$. Then

$$\bar{J}^5_k(x) = -\sigma_{ijk} \epsilon_{ijk'} H_{k'} \delta\mu.$$

We represent expression for the CSE conductivity as

$$\sigma_{ijk} = \sum_{n=-\frac{N_t}{2}}^{\frac{N_t}{2}-1} \partial_{\omega_n} \sigma^{(3)}_{ijk}, \tag{39}$$

where

$$\sigma^{(3)}_{ijk} = -\frac{1}{2\mathbf{V}} \int d^3x \int_{\mathcal{M}_3} \frac{d^3p}{(2\pi)^3} \mathrm{tr}\Big[\gamma^5 \Big[\mathbf{G}^{(0)}_W \star (\partial_{p_i} \mathbf{Q}^{(0)}_W) \star \mathbf{G}^{(0)}_W \star (\partial_{p_j} \mathbf{Q}^{(0)}_W) \star \mathbf{G}^{(0)}_W \partial_{p_k} \mathbf{Q}^{(0)}_W + 2i \mathbf{G}^{(0)}_W \star \mathbf{Q}^{(1)}_{(ij)W} \star \mathbf{G}^{(0)}_W \partial_{p_k} \mathbf{Q}^{(0)}_W - 2i \mathbf{G}^{(0)}_W \partial_{p_k} \Big[\mathbf{Q}^{(1)}_{(ij)W}\Big]\Big]\Big]. \tag{40}$$

C. The limit of small temperature

The limit of small temperature $T \to 0, N_t \to \infty, \frac{\pi}{N_t} = \epsilon \to 0$ allows us to replace the sum by an integral. The value $\omega = 0$ is to be excluded from this integral,

$$\sum_{n=-\frac{N_t}{2}}^{\frac{N_t}{2}-1} \to \frac{\beta}{2\pi} \int_{-\pi+\epsilon}^{0-\epsilon} d\omega + \frac{\beta}{2\pi} \int_{0+\epsilon}^{\pi-\epsilon} d\omega. \tag{41}$$

Then (38) becomes

$$\sigma_{ijk} = \lim_{\epsilon\to 0} \int_{-\pi+\epsilon}^{0-\epsilon} d\omega \partial_\omega \sigma^{(3)}_{ijk} + \int_{0+\epsilon}^{\pi-\epsilon} d\omega \partial_\omega \sigma^{(3)}_{ijk} = \lim_{\epsilon\to 0} \Big[\sigma^{(3)}_{ijk}(-\pi+\epsilon) - \sigma^{(3)}_{ijk}(0-\epsilon) + \sigma^{(3)}_{ijk}(0+\epsilon) - \sigma^{(3)}_{ijk}(\pi-\epsilon)\Big]. \tag{42}$$

Using $\sigma^{(3)}_{ijk}(-\pi) = \sigma^{(3)}_{ijk}(\pi)$, we obtain

$$\sigma_{ijk} = \lim_{\epsilon\to 0} \Big[\sigma^{(3)}_{ijk}(0+\epsilon) + (-\sigma^{(3)}_{ijk}(0-\epsilon))\Big], \tag{43}$$

where

$$\sigma^{(3)}_{ijk}(\omega = 0 \pm \epsilon) = -\frac{1}{2\mathbf{V}} \int d^3x \int_{\mathcal{M}_3} \frac{d^3p}{(2\pi)^4} \mathrm{tr}\Big[\gamma^5 \Big[\mathbf{G}^{(0)}_W \star (\partial_{p_i} \mathbf{Q}^{(0)}_W) \star \mathbf{G}^{(0)}_W \star (\partial_{p_j} \mathbf{Q}^{(0)}_W) \star \mathbf{G}^{(0)}_W \star \partial_{p_k} \mathbf{Q}^{(0)}_W + 2i \mathbf{G}^{(0)}_W \star \mathbf{Q}^{(1)}_{(ij)W} \star \mathbf{G}^{(0)}_W \star \partial_{p_k} \mathbf{Q}^{(0)}_W - 2i \mathbf{G}^{(0)}_W \star \partial_{p_k} \Big[\mathbf{Q}^{(1)}_{(ij)W}\Big]\Big]\Big]\Big|_{\omega=0\pm\epsilon}. \tag{44}$$

We are considering equilibrium theory, when both $\mathbf{G}$ and $\mathbf{Q}$ do not depend on time. As a result the singularities are situated at $\omega = 0$. The integrals avoid these singularities due to finite ϵ. In the absence of inhomogeneity (when the stars may be omitted in the above expressions) at $\omega = 0$ the singularities of expressions standing in the integrals mark positions of Fermi surfaces.

D. CSE conductivity as a topological invariant

Inside the integrals of Eq. (43) the two surfaces $\omega = \pm\epsilon$ cancel each other except for in the small vicinity of the singularities. Therefore, we restrict integration in Eq. (44) by the small regions (in the Brillouin zone) around the singularities. The important assumption here is the presence of precise chiral symmetry in these regions. In the other words, the continuum limit of the lattice theory under consideration is chiral invariant.

Thus γ^5 commutes/anticommutes with $\mathbf{Q}$ and $\mathbf{G}$ inside the above expression for the CSE conductivity. As a result the last two terms in Eq. (44) cancel each other, while the sum of the integrals in Eq. (43) represents a topological invariant. It does not depend on the form of the surface in the 4D momentum space surrounding the singularities. We deform this surface in such a way that it becomes small and surrounds the singularities. Therefore, instead of the two infinitely-close planes we may integrate over the sphere in the momentum space.

Thus we obtain

$$\sigma_{ijk} = -\frac{1}{2\mathbf{V}}\int_{\Sigma_3}\frac{d^3p}{(2\pi)^4}\int d^3x\,\mathrm{tr}\Big[\gamma^5\Big[\mathbf{G}_W^{(0)}\star(\partial_{p_{|i}}\mathbf{Q}_W^{(0)}) \star\mathbf{G}_W^{(0)}\star(\partial_{p_{j]}}\mathbf{Q}_W^{(0)})\star\mathbf{G}_W^{(0)}\Big]\partial_{p_k}\mathbf{Q}_W^{(0)}\Big]. \tag{45}$$

Here the integral is over Σ_3, which is the 3D hypersurface in 4D momentum space that consists of the two infinitely-close pieces of the planes. γ^5 commutes/anticommutes with $\mathbf{G}$ and $\mathbf{Q}$ in this region, and we rewrite this expression as

$$\sigma_{ijk} = -\epsilon_{ijk}\sigma_{\mathrm{CSE}}/2$$

with

$$\sigma_{\mathrm{CSE}} = \frac{\mathcal{N}}{2\pi^2} \tag{46}$$

and

$$\begin{aligned}\mathcal{N} &= \frac{\epsilon_{ijk}}{48\pi^2\mathbf{V}}\int_{\Sigma_3}d^3p\int d^3x\,\mathrm{tr}\Big[\gamma^5\Big[\mathbf{G}_W^{(0)}\star(\partial_{p_i}\mathbf{Q}_W^{(0)}) \star\mathbf{G}_W^{(0)}\star(\partial_{p_j}\mathbf{Q}_W^{(0)})\star\mathbf{G}_W^{(0)}\Big]\partial_{p_k}\mathbf{Q}_W^{(0)}\Big]\\ &= \frac{1}{48\pi^2\mathbf{V}}\int_{\Sigma_3}\int d^3x\,\mathrm{tr}\Big[\gamma^5\mathbf{G}_W^{(0)}\star d\mathbf{Q}_W^{(0)}\star\mathbf{G}_W^{(0)} \wedge\star d\mathbf{Q}_W^{(0)}\star\mathbf{G}_W^{(0)}\star\wedge d\mathbf{Q}_W^{(0)}\Big].\end{aligned} \tag{47}$$

This expression is topological invariant provided that γ^5 commutes or anticommutes with $\mathbf{Q}_W$ and $\mathbf{G}_W$ in the vicinity of Σ_3. We may deform the surface Σ_3 in such a way that it does not cross the singularities. In particular, it will acquire the form of a 3D sphere that surrounds the singularities.

In the particular case, when background is homogeneous, we obtain,

$$\mathcal{N} = \frac{1}{48\pi^2}\int_{\Sigma_3}\mathrm{tr}\Big[\gamma^5\mathbf{G}_W^{(0)}d\mathbf{Q}_W^{(0)}\mathbf{G}_W^{(0)}\wedge d\mathbf{Q}_W^{(0)}\mathbf{G}_W^{(0)}\wedge d\mathbf{Q}_W^{(0)}\Big], \tag{48}$$

where $\mathbf{Q} = \mathbf{G}^{-1}$. The index $^{(0)}$ means that magnetic field and chemical potential are set to zero to calculate the Green function. For the most simple case of the Fermi point, when chemical potential is zero, the form of Σ_3 here is an infinitely small three-dimensional sphere surrounding $p = 0$.

At zero temperature and large baryonic chemical potential the quark-gluon system may enter the quarkyonic phase with restored chiral symmetry. The increase of chemical potential may also lead to formation of color superconductivity. In the hypothetical phase, where the chiral symmetry is restored while the color superconductivity is not yet formed, the above mentioned topological invariant $\mathcal{N}$ counts the number of chiral Dirac fermions

$$\sigma_{\mathrm{CSE}} = \frac{N_c N_f}{2\pi^2},$$

where $N_c = 3$, while N_f is the number of quarks with masses smaller than μ. We then come to the standard expression for the CSE conductivity in this phase. This result, presumably, may be valid for matter existing within the neutron stars.

The above results also allow to predict the same expression for one Dirac fermion $\sigma_{\mathrm{CSE}} = \frac{1}{2\pi^2}$ in the Weyl semimetal at zero temperature. These materials are realized within solid-state physics the systems of relativistic fermions, where electronic quasiparticles are in place of quarks, while Coulomb interactions substitute the exchange by $SU(3)$ gauge bosons. These Coulomb interactions may be strong due to the electric permutivity, and additionally in these materials there are the other interactions between electrons. The result on the topological expression for the CSE conductivity does not depend on the nature of interfermions interactions. Therefore, the given topological expression remains valid in these systems as well.

IV. NONPERTURBATIVE CORRECTIONS TO CSE CONDUCTIVITY IN QCD AT FINITE TEMPERATURE

In this section we confirm the predictions of the previous sections by direct calculations using method of field

correlators developed by Yu. A. Simonov and collaborators (see also [83]).

A. Representation of axial current through the sum over quark trajectories $T > T_c$

We start from the following expression for the bare axial current at the temperature above the deconfinement crossover

$$\langle j^5_\mu(x)\rangle = \langle \mathrm{tr}_{c,D}\gamma_5\gamma_\mu S^{(\mathrm{reg})}(x,x)\rangle = \frac{\langle \mathrm{Det}(\not{D}(B,\mathcal{A})+m)\mathrm{tr}_{c,D}\gamma_5\gamma_\mu(\not{D}(B,\mathcal{A})+m)^{-1}_{xx}\rangle_B}{\langle \mathrm{Det}(\not{D}(B,\mathcal{A})+m)\rangle_B}. \tag{49}$$

Since the renormalization of the axial current operator occurs at small distances, it is the perturbative phenomenon. We neglect it here completely as we are interested in the nonperturbative contributions to the CSE conductivity originated from large distances.

For brevity we restrict ourselves in this section to the contribution of the one-quark flavor. The loop is also regularized by finite temperature; tr_c stands for the trace over color and Dirac spinor indices, respectively. $\langle\ldots\rangle_B$ stands for averaging over thermodynamic ensemble with temperature $T > T_c$, $(\beta = T^{-1})$ above the deconfinement crossover temperature $T_c \sim 160$ MeV, at nonzero baryon density that is defined with the given quark-flavor chemical potential μ, in the gluonic background field B ($B_\mu = B^a_\mu t_a$, t_a are the generators of $SU(3)$ algebra in fundamental representation), in an external constant magnetic field $\nabla\times\vec{\mathcal{A}} = \vec{H}$ directed along axis Z. Then $H_3 = \mathcal{F}_{12} =$ const is the only nonzero component of the field-strength tensor. Chemical potential is introduced as an imaginary part of the fourth component of the electromagnetic potential (in Euclidean space) $iq\mathcal{A}_4 = \mu$, where q is the electric charge of the given quark flavor.

In the following we apply quenched approximation, in which the fermion determinant is dropped. For the calculation of the quark propagator we use worldline formalism,

$$\langle j^5_\mu(x)\rangle \approx \Big\langle \mathrm{tr}_{c,D}\gamma_5\gamma_\mu(-\not{D}(B,\mathcal{A})+m)_x \times\int_0^{+\infty} ds\,\xi(s)(\overline{\mathcal{D}^4 z})^s_{xx}e^{-m^2 s-K} \times P_F P_B \exp\Big(ig\oint B\cdot dz + iq\oint\mathcal{A}\cdot dz + \int_0^s d\tau\sigma^{\rho\sigma}(gF_{\rho\sigma}(z,z_0)+q\mathcal{F}_{\rho\sigma})\Big)\Big\rangle_B, \tag{50}$$

where $\sigma_{\rho\sigma} = \frac{i}{4}[\gamma_\rho,\gamma_\sigma]$ is the generator of $SO(3,1)$. The covariant derivative is $D(B,\mathcal{A}) = \partial - igB - iq\mathcal{A}$, where g is the $SU(3)$ coupling constant. Function $\xi(s)$ regularizes the loop integral. It is needed to remove the singularity at $s = 0$. We also denote here

$$K = \int_0^s d\tau\left(\frac{\dot{z}^2(\tau)}{4}+m^2\right).$$

The path integral $(\overline{\mathcal{D}^4 z})^s_{xy}$ describes the quark motion from point x to y in worldline (proper) time s. The antiperiodic boundary conditions are assumed for the fermion when the trajectory wraps around the (imaginary) time direction. Euclidean space is taken in the form $\mathbb{R}^3\times S^1$, where the direction of imaginary time is a circle S^1 of length $\beta = T^{-1}$). The path integral discretization is implied here [76],

$$(\overline{\mathcal{D}^4 z})^s_{xy} = \lim_{N\to+\infty}\prod_{m=1}^N\frac{d^4 z_m}{(4\pi\varepsilon)^2}\sum_{n=-\infty}^{+\infty}(-1)^n\frac{d^4p}{(2\pi)^4} \times e^{(ip_\mu(\sum_{i=1}^m dz^\mu_i-(x-y)-n\beta\delta^\mu_4))}, \qquad \varepsilon = s/N. \tag{51}$$

The trace over the Dirac indices is simplified due to the presence of γ_5. We consider the leading order in the external field and use that $\mathrm{tr}_D\gamma_5\gamma_\mu\gamma_\nu\gamma_\lambda\gamma_\rho = -4\epsilon_{\mu\nu\lambda\rho}$ (in Euclidean spacetime $\{\gamma_\mu,\gamma_\nu\} = 2\delta_{\mu\nu}$). The leading order in the magnetic field is given by

$$\langle j^5_\mu(x)\rangle \approx \Big\langle \mathrm{tr}_{c,D}\gamma_5\gamma_\mu\gamma_\lambda\frac{i}{4}[\gamma_\rho,\gamma_\sigma](-D_\lambda(B,\mathcal{A}))_x \times\int_0^{+\infty} ds\xi(s)(\overline{\mathcal{D}^4 z})^s_{xx}e^{-m^2 s-K} \times P_B\exp\Big(ig\oint B\cdot dz + iq\oint\mathcal{A}\cdot dz\Big) \times\int_0^s d\tau(gF_{\rho\sigma}(z,z_0)+q\mathcal{F}_{\rho\sigma})\Big\rangle_B. \tag{52}$$

We disregard here influence of external magnetic field on configurations of gluonic fields B [75]. As a result the gluonic field correlators $\langle\ldots\rangle_B$ are isotropic. Besides, we disregard the spin-gluon interactions (these interactions do not contribute much, for example, to the string tension). Due to the definite direction of external magnetic field the Dirac indices are $(\mu\lambda[\rho\sigma] = 34[12])$. The proper time integral $\int_0^s d\tau\mathcal{F}_{12} = s\,H$ represents insertion of electromagnetic vertex at the points along quark trajectory

$$\langle j^5_\mu(x)\rangle \approx 4i\delta_{\mu 3}qH\int_0^{+\infty}\xi(s)sds\Big\langle \mathrm{tr}_c(D_4(B,\mathcal{A}))_x(\overline{\mathcal{D}^4 z})^s_{xx}e^{-m^2 s-K} \times P_B\exp\Big(ig\oint B\cdot dz + iq\oint\mathcal{A}\cdot dz\Big)\Big\rangle_B. \tag{53}$$

The covariant derivative acts on path integral. The definition of parallel transporter results in

$$(D_\lambda(B,\mathcal{A}))_x P_B \exp\left(ig\int_y^x B\cdot dz + iq\int_y^x \mathcal{A}\cdot dz\right) = 0,$$
$$z(0) = x. \tag{54}$$

As a result the covariant derivative is reduced to the ordinary one that acts on $(\overline{\mathcal{D}^4 z})^s_{xx}$. The major temperature-dependent contributions to the integral over the trajectories come from the loops that wrap n times around S^1, and we replace $\partial_4 \to \frac{\partial}{\partial(n\beta)}$. The contribution to the axial current not dependent on temperature may be neglected. At zero temperature the chiral symmetry breaking suppresses the chiral separation effect.

The electromagnetic part standing in exponent of the Wilson loop (for the quark trajectory $z^{(n)}$ that wraps n times around the temporal direction) is

$$q\oint \mathcal{A}\cdot dz^{(n)} = q\Phi_H - i\mu n\beta, \tag{55}$$

where Φ_H is the magnetic flux through the spatial projection of the loop. We are considering the linear response to the magnetic field; Eq. (53) is proportional to H, and we disregard the external magnetic field in the remaining expression. We come to the following expression

$$\begin{aligned}\langle j^5_\mu(x)\rangle &\approx 4i\delta_{\mu 3} qH\int_0^{+\infty}\xi(s)sds\prod_{m=1}^{N}\frac{d^4z_m}{(4\pi\varepsilon)^2}\sum_{n=-\infty}^{+\infty}(-1)^n\frac{d^4p}{(2\pi)^4}\frac{\partial}{\partial(n\beta)}\left(e^{(ip_\mu(\sum_{i=1}^m dz_i^\mu-(x-y)-n\beta\delta_4^\mu))}e^{-m^2s-K}\right)\\ &\times\left\langle \mathrm{tr}_c P_B\exp\left(ig\oint B\cdot dz+\mu n\beta\right)\right\rangle_B\\ &= 4i\delta_{\mu 3} qH\int_0^{+\infty}\xi(s)sds\prod_{m=1}^{N}\frac{d^4z_m}{(4\pi\varepsilon)^2}\sum_{n=-\infty}^{+\infty}(-1)^n\frac{d^4p}{(2\pi)^4}\frac{\partial}{\partial(n\beta)}\left(e^{(ip_\mu(\sum_{i=1}^m dz_i^\mu-(x-y)-n\beta\delta_4^\mu))}e^{-m^2s-K}\right)\\ &\times\left\langle \mathrm{tr}_c P_B\exp\left(ig\oint B\cdot dz+\mu n\beta\right)\right\rangle_B.\end{aligned} \tag{56}$$

The last expression allows us to represent the CSE conductivity $\frac{\partial}{\partial\mu}\frac{\partial}{\partial H_k}\langle j^5_k(x)\rangle$ as

$$\begin{aligned}\sigma_{\mathrm{CSE}} &\approx 4i\int_0^{+\infty}\xi(s)sds\prod_{m=1}^{N}\frac{d^4dz_m}{(4\pi\varepsilon)^2}\sum_{n=-\infty}^{+\infty}(-1)^n\frac{d^4p}{(2\pi)^4}\left\langle \mathrm{tr}_c P_B\exp\left(ig\oint B\cdot dz\right)\right\rangle_B e^{\mu n\beta}\\ &\times\frac{\partial}{\partial(\log\beta)}e^{-m^2s-K+(ip_\mu(\sum_{i=1}^m dz_i^\mu-(x-y)-n\beta\delta_4^\mu))}.\end{aligned} \tag{57}$$

B. Evaluation of integral over quark trajectories

Below we adopt the version of the Simonov technique proposed in [84]. It is based on the Abelian-Diakonov-Petrov representation of the Wilson loop. In this representation we obtain the following expression for quark condensate (which is a function of the bare mass m, temperature, and chemical potential)

$$\begin{aligned}\sigma_{\mathrm{CSE}} &\approx -4iN_c\frac{\partial}{\partial m^2}\int_0^{+\infty}\xi(s)ds\prod_{m=1}^{N}\frac{d^4dz_m}{(4\pi\varepsilon)^2}\sum_{n=-\infty}^{+\infty}(-1)^n\frac{d^4p}{(2\pi)^4}e^{\mu n\beta}\\ &\times\frac{\partial}{\partial(\log\beta)}\left(e^{-m^2s-K+(ip_\mu(\sum_{i=1}^m dz_i^\mu-(x-y)-n\beta\delta_4^\mu))}\right)\times\left\langle\exp\left(ig\oint\mathcal{B}\cdot dz\right)\right\rangle_B.\end{aligned} \tag{58}$$

Here the kernel K is redefined as

$$K = \int_0^s d\tau\left(\frac{\dot z^2(\tau)}{4}+m^2\right)-\kappa\int_0^s\sqrt{\dot z^2(\tau)}d\tau.$$

Constant κ entering this expression contains ultraviolet divergency, and is to be absorbed by the renormalization of the quark mass. The Abelian field $\mathcal{B}$ is defined as the component of the $SU(3)$ gauge field (taken in the fundamental representation),

$$\mathcal{B}_\mu = B^{11}_\mu.$$

In this Abelian representation, the Wilson loop $\mathcal{C}$ factorizes in the simply-connected loop $\mathcal{C}_l$ (the one, which does not wrap along the S^1), and the straight Polyakov line $\mathcal{L}^{(n)}$ that is wrapped n-times along the S^1

$$\langle W[\mathcal{C}]\rangle_B = \langle W[\mathcal{C}_l] W[\mathcal{L}^{(n)}]\rangle_B, \tag{59}$$

where

$$W[\mathcal{C}] = \exp\left(ig \oint_{\mathcal{C}} \mathcal{B}\cdot dz \right).$$

Following [77] we neglect the correlation between the Polyakov line and the remaining part of the Wilson loop. This results in

$$\langle W[\mathcal{C}]\rangle_B \approx \langle W[\mathcal{C}_l]\rangle_B L^{(n)}, L^{(n)} \approx L^{|n|} \tag{60}$$

and

$$L^{(n)} = \exp\left(ig \oint_{\mathcal{L}^{(n)}} \mathcal{B}\cdot dz \right).$$

The Polyakov line determines potential V_1

$$L = \exp\left(-\frac{V_1(r\to+\infty, T)}{2T} \right),$$
$$V_1(r\to+\infty, T) = V_1(T) = V_1, \tag{61}$$

where V_1 is energy required to overcome the remnant interaction that bounds the quark as a part of a color-singlet state. This potential was not yet calculated within the method of field correlators, and we use here the lattice data [25]

$$V_1(T > T_c) = \frac{175\ \text{MeV}}{1.35T/T_c - 1},$$
$$V_1(T_c) = 0.5\ \text{GeV}, \qquad T_c = 160\ \text{MeV}. \tag{62}$$

For the sake of rough evaluation we substitute $W[\mathcal{C}_l]$ by its spatial projection with the dominant contribution given by color-magnetic confinement $W[\mathcal{C}_l] \sim \exp(-\sigma_H S_3[\vec{z}])$, where S_3 is the minimal area spanned on the spatial projection of Wilson loop. Effectively, the color-magnetic confinement results in the appearance of the thermal-quark mass

$$m \to \sqrt{m^2 + m_D^2/4}, \qquad m_D^2 = c_D^2 \sigma_H(T),$$
$$\sigma_H(T) \approx c_\sigma^2 g^4(T,\mu) T^2, \tag{63}$$

where $c_D \approx 2$ and $c_\sigma \approx 0.56$ are numerical constants that are taken from the analysis of the experimental consequences of the thermal mass appearance. Those values are extracted from lattice data in Ref. [79]. For $T \approx \mu \approx T_c$ we have $m_D/2 \approx 320$ MeV.

However, nonperturbative "perimeter-law" contribution to quark self-energy shifts down the effective quark mass. Let us adapt the result of [85] for the quark propagator to the deconfined phase

$$\Delta m^2 = -\Lambda = -\int d^4(y-x) \times \langle \sigma_{\mu\nu} F^{\mu\nu}(x) \Phi_{xy} \sigma_{\mu'\nu'} F^{\mu'\nu'}(y) \Phi_{yx}\rangle_B G(x,y). \tag{64}$$

In the deconfined phase the color-electric confining correlator is absent while the color-magnetic is present (in fact, we neglect all the correlators $D_1^{E,H,EH}$ but D^H) $\langle \sigma_{\mu\nu} F^{\mu\nu}(x) \times \Phi_{xy} \sigma_{\mu'\nu'} F^{\mu'\nu'}(y) \Phi_{yx}\rangle \approx \langle \sigma_{ij} F^{ij}(x) \Phi_{xy} \sigma_{i'j'} F^{i'j'}(y) \Phi_{yx}\rangle$.

Since the QCD vacuum-correlation length $\lambda \sim 1\ \text{GeV}^{-1} \ll \beta$ (in the old paper [85] the length is denoted as T_g) in temperature range which we find interesting, the integral for the nonperturbative self-energy converges within one winding. Also, the current quark masses for the light flavors are small in comparison to the inverse correlation length. Thus, we approximate the exact squared propagator in the external magnetic field G in (64) with the free-scalar propagator.

The consideration of [85] is applicable up to the overall spin-averaging factor; the factor $\sigma_{\mu\nu}\sigma^{\mu\nu} = D(D-1)/4$ in the confined phase is to be replaced with $\sigma_{ij}\sigma^{ij} = (D-1)(D-2)/4$. Thus, the quark mass shift Δm_q^2 in the QGP phase is twice smaller then in the hadronic phase. Finally, the resulting effective quark mass M is

$$\Delta m^2 \approx -\frac{2}{\pi}\sigma_H(T), \tag{65}$$

$$M^2 = m^2 + (c_D^2/4 - 2/\pi)\sigma_H(T). \tag{66}$$

The correction reduces the screened quark mass (63) by a factor $\sqrt{1-\frac{2}{\pi}} \sim \frac{2}{3}$. In particular, we then have $m_D/2 \approx 200$ MeV for $T \approx \mu \approx T_c$.

The effect of the appearance of thermal mass may be taken into account (roughly) if the integration over the spatial coordinates of the quark trajectories is performed as for the free particle, but with the current mass m substituted by M (see Refs. [77–79]). We set $K_3 = \int_0^s d\tau \dot{\vec{z}}^2/4$, and obtain,

$$\int (\mathcal{D}^3\vec{z})_{\vec{x},\vec{x}}^{s} e^{-K_3 - m^2 s} \left\langle \exp\left(ig \oint \vec{\mathcal{B}}\cdot d\vec{z} \right) \right\rangle_B \sim \frac{e^{-M^2 s}}{(4\pi s)^{3/2}}. \tag{67}$$

The running coupling may be evaluated in one loop as

$$g^2(T,\mu) = \frac{1}{2b_0 \log \frac{\sqrt{T^2 + 3\mu^2/\pi^2}}{T_c L_\sigma}}, \qquad (4\pi)^2 b_0 = \frac{11}{3}N_c - \frac{2}{3}N_f, \tag{68}$$

with $L_\sigma \approx 0.1$. The numerical estimate for temperature and chemical potential around T_c is

$$\alpha_s(T_c, T_c) \approx 0.29.$$

This demonstrates that the perturbative corrections may, in principle, change the result by about 30%.

The calculation of the integral over the temporal part of the quark trajectories takes into account the nonzero value of the Polyakov line. Here we denote $K_4 = \int_0^s d\tau \dot{z}_4^2/4$,

$$\int (\mathcal{D}z_4)^s_{0,n\beta} e^{-K_4} \left\langle \exp\left(ig \int \mathcal{B}_4 dz_4 + iq \int \mathcal{A}_4 dz_4 \right) \right\rangle_B \approx \frac{e^{-\frac{n^2\beta^2}{4s}}}{\sqrt{4\pi s}} L^{|n|} \exp(\mu n \beta). \tag{69}$$

In the Appendix we represent, for comparison, the calculation of path integral for the free fermions.

Following [77] we conclude that here the result for the free fermions is to be used, where we substitute (instead of the current mass of quark) its thermal (Debye) mass and the Polyakov line. We combine Eqs. (67) and (69) to calculate the CSE conductivity,

$$\sigma_{\rm CSE} \approx -\frac{\partial}{\partial M^2} \frac{N_c}{2\pi^2} \int_0^{+\infty} \frac{ds}{s^2} \sum_{n=1}^{+\infty} (-1)^n \cosh(\mu n\beta) L^n \frac{\partial}{\partial(\log\beta)} \times \exp\left(-M^2 s - \frac{n^2\beta^2}{4s} \right). \tag{70}$$

In this expression only the nonperturbative contributions are taken into account. The subdominant perturbative contributions are neglected here. The nonwinding trajectories, $n = 0$, are not taken into account since this divergent contribution is T- and μ-independent "vacuum density" [36]. Its derivative does not give contributions to $\sigma_{\rm CSE}$. Now the regularization $\xi(s)$ is no longer needed.

C. Evaluation of $\sigma_{\rm CSE}$

We use integral representations for the modified Bessel functions,

$$K_\nu(z) = \frac{1}{2}\left(\frac{z}{2}\right)^\nu \int_0^{+\infty} \exp\left(-t - \frac{z^2}{4t} \right) \frac{dt}{t^{\nu+1}}, \tag{71}$$

$$K_0'(z) = -K_1(z), \tag{72}$$

$$K_\nu(z) = \frac{\sqrt{\pi}(z/2)^\nu}{\Gamma(\nu + \frac{1}{2})} \int_0^{+\infty} e^{-z\cosh t} (\sinh t)^{2\nu} dt. \tag{73}$$

To use the first expression we substitute $s = M^2 t$,

$$\sigma_{\rm CSE} \approx -\frac{\partial}{\partial M^2} \frac{2M^2 N_c}{\pi^2} \sum_{n=1}^{+\infty} (-1)^n \cosh(\mu n\beta) L^n \times \frac{\partial}{\partial \log\beta} \frac{K_1(n\beta M)}{n\beta M}. \tag{74}$$

Then we use the second representation

$$\sigma_{\rm CSE} \approx -\frac{\partial}{\partial M^2} \frac{2M^2 N_c}{\pi^2} \sum_{n=1}^{+\infty} (-1)^n \cosh(\mu n\beta) L^n \times \frac{\partial}{\partial \log\beta} \int_0^{\infty} e^{-n\beta M \cosh t} \sinh^2 t dt \tag{75}$$

and substitute $p = M \sinh t$. As a result we get

$$\begin{aligned}
\sigma_{\rm CSE} &\approx \frac{\partial}{\partial M^2} \frac{N_c}{\pi^2} \sum_{n=1}^{+\infty} (-1)^n \int_0^{+\infty} p^2 dp \left(e^{\beta n(\mu - V_1/2 - \sqrt{p^2+M^2})} \beta n + (\mu \to -\mu) \right) \\
&= -\frac{N_c}{2\pi^2} \sum_{n=1}^{+\infty} (-1)^n \int_0^{+\infty} \frac{p^2 dp}{\sqrt{p^2+M^2}} \left(e^{\beta n(\mu - V_1/2 - \sqrt{p^2+M^2})} (\beta n)^2 + (\mu \to -\mu) \right) \\
&= -\frac{\partial^2}{\partial \mu^2} \frac{N_c}{2\pi^2} \sum_{n=1}^{+\infty} (-1)^n \int_0^{+\infty} \frac{p^2 dp}{\sqrt{p^2+M^2}} \left(e^{\beta n(\mu - V_1/2 - \sqrt{p^2+M^2})} + (\mu \to -\mu) \right).
\end{aligned} \tag{76}$$

The sum is calculated as geometrical progression, which yields Fermi-Dirac distribution $f_\beta(\varepsilon) = (e^{\beta\varepsilon} + 1)^{-1}$,

$$\begin{aligned}
\sigma_{\rm CSE} &\approx \frac{\partial}{\partial M^2} \frac{\partial}{\partial \mu} \frac{N_c}{\pi^2} \sum_{n=1}^{+\infty} (-1)^n \int_0^{+\infty} p^2 dp \left(e^{\beta n(\mu - V_1/2 - \sqrt{p^2+M^2})} - (\mu \to -\mu) \right), \\
&= -\frac{\partial}{\partial M^2} \frac{\partial}{\partial \mu} \frac{N_c}{\pi^2} \int_0^{+\infty} p^2 dp (f_\beta(\mathcal{E}_M(p) + V_1/2 - \mu) - f_\beta(\mu \to -\mu)), \\
&= \frac{\partial^2}{\partial \mu^2} \frac{N_c}{2\pi^2} \int_0^{+\infty} \frac{p^2 dp}{\sqrt{p^2+M^2}} (f_\beta(\mathcal{E}_M(p) + V_1/2 - \mu) + f_\beta(\mu \to -\mu)),
\end{aligned} \tag{77}$$

where $\mathcal{E}_M(p) = \sqrt{p^2 + M^2}$. One can easily see that in the limiting case $\mu \gg T$,

$$\sigma_{\mathrm{CSE}} = \frac{\partial}{\partial M^2}\frac{N_c}{\pi^2}\int_0^{+\infty} p^2 dp \delta(\mathcal{E}_M(p) + V_1/2 - \mu) = \frac{N_c}{2\pi^2} \tag{78}$$

as expected. Our numerical results are represented in Figs. 2–4. The dependence of Eq. (79) on μ is represented in Fig. 4. It is worth mentioning that strictly speaking at $\mu \gg T_c$ the above expressions for V_1 and M cannot be applied. As expected both these quantities decrease essentially with an increase of μ. As a result, the value of σ_{CSE}, approaches the conventional value faster than represented in Fig. 4.

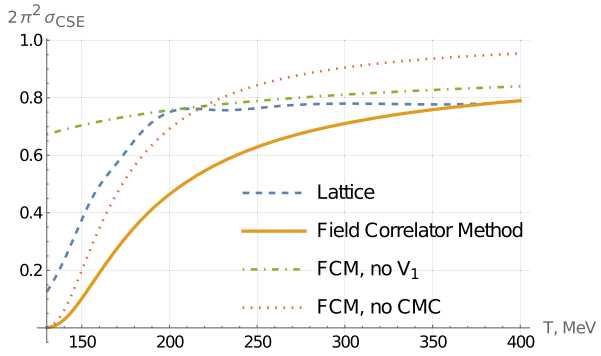

FIG. 2. We represent here the comparison of our nonperturbative calculation (79) using method of field correlators with the lattice numerical simulations taken from [49] calculated on the lattices $24^3 \times 6$ and $24^3 \times 8$. The plot represents the data on $2\pi\sigma_{\mathrm{CSE}}$ (per Dirac fermion, i.e., divided by the number of quark flavors N_f and colors N_c) at $\mu = 0$. The dashed line represents lattice data. Solid line represents the results obtained via the field-correlator method (FCM). Besides, we represent here the results obtained using two modifications of the FCM; the dotted line represents results with the thermal quark mass disregarded, i.e., without color-magnetic confinement (CMC), while the dashed-dotted line represents the results with the Polyakov-line contribution V_1 disregarded.

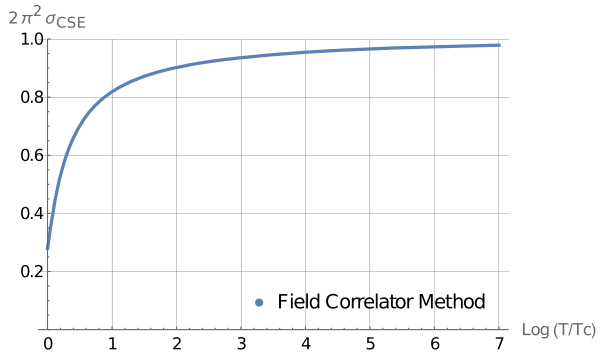

FIG. 3. We represent here the dependence of $2\pi\sigma_{\mathrm{CSE}}$ (per Dirac fermion, i.e divided by the number of quark flavors N_f and colors N_c) (79) at $\mu = T_c$ as a function of T.

In Fig. 2 we compare our results with those obtained using lattice numerical simulations. One can see that qualitatively the two methods give similar results. Quantitative difference may be caused by several factors. First of all, the finite volume effects may be strong for the lattice simulations with given lattice sizes. Next, perturbative corrections disregarded in our calculations may change the results. Also, our result heavily depends on an 'unstable' numerical input $V_1(T)$ (62). One can see that at small temperatures the FCM gives results that match lattice data if thermal mass is neglected, while at large temperatures the FCM matches lattice results if thermal mass is taken into account while Polyakov-line contribution is neglected. The complete FCM interpolates between the two.

Looking at the results presented in Fig. 4 we conclude that at the values of quark chemical potential accessed at LHC, RHIC, NICA, and FAIR the topological regime is not yet achieved, and the CSE conductivity is suppressed essentially compared to the standard topological value.

In addition in Fig. 3 we represent the dependence of σ_{CSE} in units of $\frac{N_c N_f}{2\pi^2}$ at $\mu = T_c$ as a function of temperature. One can see that this value approaches the conventional one only at the electroweak scale $T \sim 100$ GeV.

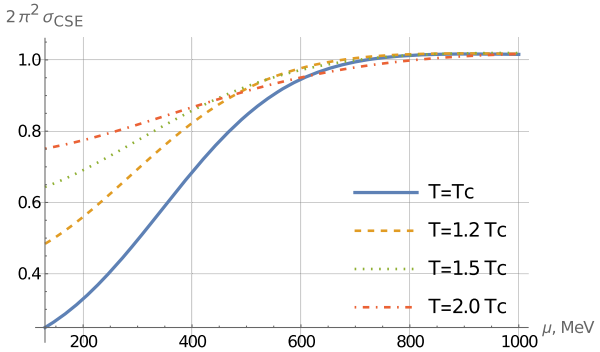

FIG. 4. We represent here our data on $2\pi\sigma_{\mathrm{CSE}}$ (per Dirac fermion) (79) as a function of μ at various temperatures.

V. CONCLUSIONS AND DISCUSSION

In the present paper we consider effect of interactions on the chiral separation effect. First of all, we are interested in the effect of strong interactions on the CSE in quark matter. However, the obtained zero temperature results may be applied directly to the CSE in Weyl semimetals as well.

We prove that in the fermion system with chiral symmetry at zero temperature in the presence of an external magnetic-field strength F_{ij} and chemical potential μ, the derivative of the renormalized axial current averaged over the overall volume is given by

$$\frac{d\bar{J}_5^k}{d\mu} = \frac{\mathcal{N}}{4\pi^2}\epsilon^{ijk0}F_{ij}. \tag{79}$$

(By renormalized current we understand expression with the bare-velocity operator substituted by the renormalized one.) This expression is valid provided that $\lambda^2|F_{ij}| \ll 1$, where λ is the correlation length of the given system. In particular, for homogeneous cold quark matter with $\mu > \Lambda_{\mathrm{QCD}}$ we need magnetic field strength much smaller than Λ^2_{QCD}.

Here $\mathcal{N}$ is the topological invariant given by

$$\mathcal{N} = \frac{1}{48\pi^2\mathbf{V}}\int_{\Sigma_3}\int d^3x\,\mathrm{tr}[\gamma^5\mathbf{G}_W^{(0)}\star d\mathbf{Q}_W^{(0)}\star\mathbf{G}_W^{(0)} \wedge \star d\mathbf{Q}_W^{(0)}\star\mathbf{G}_W^{(0)}\star \wedge d\mathbf{Q}_W^{(0)}]. \tag{80}$$

In this expression $\hat{\mathbf{G}}^{(0)}$ is the renormalized complete two-point Green function with interaction corrections included. It has to be calculated after a certain gauge is fixed (if we are speaking of the quark matter). The result does not depend on the chosen gauge; $\mathbf{G}_W^{(0)}$ is its Wigner transformation. Correspondingly, $\hat{\mathbf{Q}}^{(0)}$ is operator inverse to $\hat{\mathbf{G}}^{(0)}$, while $\mathbf{Q}_W^{(0)}$ is its Weyl symbol. Superscript $^{(0)}$ means that the expression for $\hat{\mathbf{G}}$ does not contain the external magnetic field. The surface Σ_3 in momentum space depends on x and surrounds the hypersurface of the singularities of the expression standing inside the integral. The latter hypersurface generalizes the notion of the Fermi surface and reduces to it in the homogeneous case. It is supposed that at $\Sigma_3(x)$ for any x matrix γ^5 commutes (or anticommutes) with both $\mathbf{G}_W^{(0)}$ and $\mathbf{Q}_W^{(0)}$. (Correspondingly, in the homogenous system this requirement means that γ^5 commutes/anticommutes with $\mathbf{G}^{(0)}$ at the Fermi surface.) This means, actually, that in the given system at low energies there is chiral symmetry. In the system with N chiral Dirac fermions $\mathcal{N} = N$, and the above result means that the CSE conductivity is given by

$$\sigma_{\mathrm{CSE}} = \frac{N}{2\pi^2}.$$

Being applied to the quark-gluon matter this means that if the dense cold quark matter exists in the phase with restored chiral symmetry without color superconductivity (we also neglect effect of instantons), then in this phase the chiral separation effect is present with the conventional expression for the CSE conductivity. The same refers to the quark-gluon plasma phase provided that $\mu \gg T$. We calculate directly the nonperturbative corrections to the CSE conductivity at a finite temperature above the deconfinement phase transition. Our results confirm that σ_{CSE} approaches the conventional expression at large μ for any given $T > T_c$. However, in the region of the phase diagram accessible at the modern colliders the topological expression for σ_{CSE} is not yet approached, and the conductivity is essentially suppressed. It is worth mentioning that at $\mu, T \sim T_c$ the perturbative corrections will give contributions of the order of 30% since $\alpha_s(T_c) \approx 0.3$. At the same time for large μ the perturbative corrections are already not so relevant because α_s decreases with the increase of μ. Nevertheless, the calculation of the perturbative corrections to σ_{CSE} is worth performing, but this is out of the scope of the present paper.

The obtained results may also be applied to the CSE in Weyl semimetals, where electronic quasiparticles are subject to Coulomb interactions. Those interactions are typically strong because the effective finite-structure constant is of the order of unity. Left and right-handed fermions in momentum space are separated here in momentum space. The boundary of the samples contain Fermi arcs. In the presence of a magnetic field and a chemical potential that exceeds the level of Fermi points, the axial current appears. Then the left- and the right-handed electrons move in opposite directions. As a result, at the boundary of the sample there will be excess of the electrons at the left-handed Weyl point and a deficiency of the electrons at the right-handed Weyl point (or vice versa). This results in the appearance of the Fermi pockets instead of the Fermi arcs (electron Fermi pocket close to one of the Weyl points, and hole pocket close to the other Weyl point). This is how the CSE effect may be observed experimentally in these materials.

It is worth mentioning that the perturbative calculation of corrections to the CSE conductivity in pure QED performed in [53] suggests the appearance of a correction proportional to fine-structure constant $\alpha \approx 1/137$, and containing the infrared divergencies. Our approach may be applied effectively to pure QED as well. The essential difference between the two approaches is that in the present paper from the very beginning the renormalized axial current is calculated according to Sec. II D. This approach takes into account the renormalization procedure both for the propagators and for the interaction vertices automatically. In [53] corrections to the bare-axial current are calculated. Presumably, the renormalization procedure applied to the expression given in [53] will remove radiative corrections to the CSE conductivity completely.

The cousin of the CSE—the chiral vortical effect (CVE)—is expected in quark matter under the same conditions as the CSE, i.e., in the same region of the QCD phase diagram. The rotating fireballs containing quark-gluon plasma appear during the noncentral heavy-ion collisions. The interior of neutron stars may contain quark matter in the phase with restored chiral symmetry. Above we mentioned that this phase might exist without color superconductivity. Rotation results in the appearance of axial current along the axis of rotation in quark systems, and at zero temperature, rotation may effectively be described by the effective Abelian gauge field μu_k, where u_k is the four-vector of rotation velocity [86]. As a result the CVE is reduced to CSE, and the axial current is given by

$$J_5 = \frac{\mathcal{N}}{2\pi^2}\mu^2\Omega.$$

Here Ω is angular velocity while $\mathcal{N}$ is given by Eq. (80). In cold quark matter $\mathcal{N} = N_c N_f$, where N_f is the number of quarks with masses smaller than μ. The same expression might also be applied to quark gluon plasma at $\mu \gg T$ if the rotation is considered as rigid. (Actually, the fireballs do not rotate rigidly.) Therefore, this approach may be taken into account only qualitatively. In the domain $\mu \sim T$ the mentioned methodology, in which rotation is introduced through the effective Abelian gauge field, cannot be applied at all. Namely, rotation of thermal quasiparticles cannot be described by the effective Abelian gauge field. Rotating thermal quasiparticles contribute the axial current along the axis of rotation; these contributions should be taken into account separately. Notice that in [87,88] it has been pointed out that the temperature depending term in the CVE conductivity does receive interaction corrections resulted from the exchange by gauge bosons. However, in [87] it was argued that this term is not subject to corrections resulted from Yukawa interactions.

APPENDIX

We present here the calculation of quark propagator using method of the main text applied to the noninteracting system at finite temperature. This way we check the normalization factor entering the measure in the path integral over trajectories (51),

$$-S(x,y) = (\not{\partial} - m)G(x,y), \tag{A1}$$

$$G(x,y) = \int_0^{+\infty} ds (\overline{\mathcal{D}^4 z})^s_{xy} \exp\left(-m^2 s - \frac{1}{4}\int_0^s \dot{z}^2 d\tau\right) \tag{A2}$$

$$\begin{aligned} &= \int_0^{+\infty} ds \lim_{\substack{N\to+\infty \\ \varepsilon = s/N}} \left(\prod_{m=1}^{N} \frac{d^4 z_m}{(4\pi\varepsilon)^2}\right) \sum_{n=-\infty}^{+\infty} (-1)^n \frac{d^4 p}{(2\pi)^4} \exp\left(ip_\mu \left(\sum_{i=1}^{N} dz_i^\mu - (x-y)^\mu - n\beta\delta_4^\mu\right) - m^2 s - \sum_{i=1}^{N}\frac{dz_i^2}{4\varepsilon}\right) \\ &= \int_0^{+\infty} ds \sum_{n=-\infty}^{+\infty} (-1)^n \int \frac{d^4 p}{(2\pi)^4} \exp\left(-(p^2+m^2)s - ip\cdot(x-y) - ip_4 n\beta\right) \\ &= \sum_{n=-\infty}^{+\infty} (-1)^n \int \frac{d^4 p}{(2\pi)^4} \frac{\exp\left(-ip\cdot(x-y) - ip_4 n\beta\right)}{p^2+m^2}. \end{aligned} \tag{A3}$$

The antiperiodic boundary conditions in imaginary time are assumed here [89]

$$(\not{\partial} + m)S(x) = \delta(x), \qquad S(\tau+\beta,\vec{x}) = -S(\tau,\vec{x}). \tag{A4}$$

In coordinate representation the propagator reads

$$G(x,y) = \sum_{n=-\infty}^{+\infty} (-1)^n \int_0^{+\infty} \frac{ds}{(4\pi s)^2} \exp\left(-m^2 s - \frac{z_n^2}{4s}\right). \tag{A5}$$

This gives

$$G(x,y) = \sum_{n=-\infty}^{+\infty} (-1)^n \frac{m}{4\pi^2 z_n} K_1(m z_n), \tag{A6}$$

where $z_n^2 = (\vec{x}-\vec{y})^2 + (x_4 - y_4 + n\beta)^2$.

[1] M. A. Metlitski and A. R. Zhitnitsky, Anomalous axion interactions and topological currents in dense matter, Phys. Rev. D **72**, 045011 (2005).

[2] D. E. Kharzeev, The Chiral Magnetic Effect and anomaly-induced transport, Prog. Part. Nucl. Phys. **75**, 133 (2014).

[3] D. E. Kharzeev, J. Liao, S. A. Voloshin, and G. Wang, Chiral magnetic effect in high-energy nuclear collisions—A status report, Prog. Part. Nucl. Phys. **88**, 1 (2016).

[4] D. E. Kharzeev, Chern-simons current and local parity violation in hot QCD matter, Nucl. Phys. **A830**, 543c (2009).

[5] L. P. Csernai, V. K. Magas, and D. J. Wang, Flow vorticity in peripheral high energy heavy ion collisions, Phys. Rev. C **87**, 034906 (2013).

[6] V. A. Miransky and I. A. Shovkovy, Quantum field theory in a magnetic field: From quantum chromodynamics to graphene and Dirac semimetals, Phys. Rep. **576**, 1 (2015).

[7] K. Landsteiner, E. Megias, and F. Pena-Benitez, Anomalous transport from Kubo formulae, Lect. Notes Phys. **871**, 433 (2013).

[8] S. Parameswaran, T. Grover, D. Abanin, D. Pesin, and A. Vishwanath, Probing the Chiral Anomaly with Nonlocal Transport in Weyl Semimetals, Phys. Rev. X **4**, 031035 (2014).

[9] E. V. Gorbar, V. A. Miransky, I. A. Shovkovy, and P. O. Sukhachov, Chiral separation and chiral magnetic effects in a slab: The role of boundaries, Phys. Rev. B **92**, 245440 (2015).

[10] V. A. Miransky and I. A. Shovkovy, Quantum field theory in a magnetic field: From quantum chromodynamics to graphene and Dirac semimetals, Phys. Rep. **576** (2015).

[11] S. N. Valgushev, M. Puhr, and P. V. Buividovich, Chiral magnetic effect in finite-size samples of parity-breaking Weyl semimetals, Proc. Sci. LATTICE2015 (**2015**) 043 [arXiv:1512.01405].

[12] P. V. Buividovich, M. Puhr, and S. N. Valgushev, Chiral magnetic conductivity in an interacting lattice model of parity-breaking Weyl semimetal, Phys. Rev. B **92**, 205122 (2015).

[13] P. V. Buividovich, Spontaneous chiral symmetry breaking and the chiral magnetic effect for interacting Dirac fermions with chiral imbalance, Phys. Rev. D **90**, 125025 (2014).

[14] P. V. Buividovich, Anomalous transport with overlap fermions, Nucl. Phys. **A925**, 218 (2014).

[15] K. Fukushima and T. Hatsuda, The phase diagram of dense QCD, Rep. Prog. Phys. **74**, 014001 (2011).

[16] A. V. Smilga, Physics of thermal QCD, Phys. Rep. **291**, 106 (1997).

[17] K. Rajagopal and F. Wilczek, *The Condensed Matter Physics of QCD* (World Scientific, 2001).

[18] D. H. Rischke, The quark-gluon plasma in equilibrium, Prog. Part. Nucl. Phys. **52**, 197 (2004).

[19] M. G. Alford, A. Schmitt, K. Rajagopal, and T. Schafer, Color superconductivity in dense quark matter, Rev. Mod. Phys. **80**, 1455 (2008).

[20] R. S. Hayano and T. Hatsuda, Hadron properties in the nuclear medium, Rev. Mod. Phys. **82**, 2949 (2010).

[21] M. Huang, QCD phase diagram at high temperature and density, arXiv:1001.3216.

[22] J. O. Andersen, W. R. Naylor, and A. Tranberg, Phase diagram of QCD in a magnetic field: A review, Rev. Mod. Phys. **88**, 025001 (2016).

[23] K. Fukushima and C. Sasaki, The phase diagram of nuclear and quark matter at high baryon density, Prog. Part. Nucl. Phys. **72**, 99 (2013).

[24] A. R. Zhitnitsky, QCD as a topologically ordered system, Ann. Phys. (Amsterdam) **336**, 462 (2013).

[25] Y. A. Simonov and M. A. Trusov, Vacuum phase transition at nonzero baryon density, Phys. Lett. B **650**, 36 (2007).

[26] M. I. Krivoruchenko, D. K. Nadyozhin, T. L. Rasinkova, Y. A. Simonov, M. A. Trusov, and A. V. Yudin, Nuclear matter at high density: Phase transitions, multiquark states, and supernova outbursts, Phys. At. Nucl. **74**, 371 (2011).

[27] M. Vazifeh and M. Franz, Electromagnetic Response of Weyl Semimetals, Phys. Rev. Lett. **111**, 027201 (2013).

[28] Y. Chen, S. Wu, and A. Burkov, Axion response in Weyl semimetals, Phys. Rev. B **88**, 125105 (2013).

[29] Y. Chen, D. Bergman, and A. Burkov, Weyl fermions and the anomalous Hall effect in metallic ferromagnets, Phys. Rev. B **88**, 125110 (2013).

[30] S. T. Ramamurthy and T. L. Hughes, Patterns of electromagnetic response in topological semi-metals, Phys. Rev. B **92**, 085105 (2015).

[31] A. A. Zyuzin and A. A. Burkov, Topological response in Weyl semimetals and the chiral anomaly, Phys. Rev. B **86**, 115133 (2012).

[32] P. Goswami and S. Tewari, Axionic field theory of $(3+1)$-dimensional Weyl semi-metals, Phys. Rev. B **88**, 024510 (2013).

[33] C.-X. Liu, P. Ye, and X.-L. Qi, Chiral gauge field and axial anomaly in a Weyl semimetal, Phys. Rev. B **87**, 235306 (2015).

[34] G. B. Cook, S. L. Shapiro, and S. A. Teukolsky, Rapidly rotating neutron stars in general relativity: Realistic equations of state, Astrophys. J. **424**, 823 (1994).

[35] M. Suleymanov and M. A. Zubkov, Chiral separation effect in nonhomogeneous systems, Phys. Rev. D **102**, 076019 (2020).

[36] A. Vilenkin, Equilibrium parity-violating current in a magnetic field, Phys. Rev. D **22**, 3080 (1980).

[37] K. Fukushima, D. E. Kharzeev, and H. J. Warringa, Chiral magnetic effect, Phys. Rev. D **78**, 074033 (2008).

[38] D. E. Kharzeev and H. J. Warringa, Chiral magnetic conductivity, Phys. Rev. D **80**, 034028 (2009).

[39] D. T. Son and N. Yamamoto, Berry Curvature, Triangle Anomalies, and Chiral Magnetic Effect in Fermi Liquids, Phys. Rev. Lett. **109**, 181602 (2012).

[40] M. A. Zubkov, Wigner transformation, momentum space topology, and anomalous transport, Ann. Phys. (Amsterdam) **373**, 298 (2016).

[41] M. A. Zubkov, Absence of equilibrium Chiral Magnetic Effect, Phys. Rev. D **93**, 105036 (2016).

[42] M. M. Vazifeh and M. Franz, Electromagnetic Response of Weyl Semimetals, Phys. Rev. Lett. **111**, 027201 (2013).

[43] N. Yamamoto, Generalized Bloch theorem and chiral transport phenomena, Phys. Rev. D **92**, 085011 (2015).

[44] C. Banerjee, M. Lewkowicz, and M. A. Zubkov, Equilibrium chiral magnetic effect: Spatial inhomogeneity, finite temperature, interactions, Phys. Lett. B **819**, 136457 (2021).

[45] C. Banerjee, M. Lewkowicz, and M. A. Zubkov, Chiral magnetic effect out of equilibrium, Phys. Rev. D **106**, 074508 (2022).
[46] H. B. Nielsen and M. Ninomiya, Adler-Bell-Jackiw anomaly and Weyl fermions in crystal, Phys. Lett. **130B**, 389 (1983).
[47] Q. Li, D. E. Kharzeev, C. Zhang, Y. Huang, I. Pletikosic, A. V. Fedorov, R. D. Zhong, J. A. Schneeloch, G. D. Gu, and T. Valla, Chiral magnetic effect in $ZrTe_5$, Nat. Phys. **12**, 550.
[48] Z. V. Khaidukov and M. A. Zubkov, Chiral separation effect in lattice regularization, Phys. Rev. D **95**, 074502 (2017).
[49] B. B. Brandt, F. Cuteri, G. EndrHodi, E. G. Velasco, and G. Mark'o, Anomalous transport phenomena on the lattice, Proc. Sci. LATTICE2022 (**2023**) 173 [arXiv:2212.02148].
[50] T. D. Lee and M. Nauenberg, Degenerate systems and mass singularities, Phys. Rev. B **133**, 1549 (1964).
[51] T. Kinoshita, Mass singularities of Feynman amplitudes, J. Math. Phys. (N.Y.) **3**, 650 (1962).
[52] G. Sterman and S. Weinberg, Jets from Quantum Chromodynamics, Phys. Rev. Lett. **39**, 1436 (1977).
[53] E. V. Gorbar *et al.*, Radiative corrections to chiral separation effect in QED, Phys. Rev. D **88**, 025025 (2013).
[54] H. Weyl, Quantenmechanik und gruppentheorie, Z. Phys. **46**, 1 (1927).
[55] E. P. Wigner, On the quantum correction for thermodynamic equilibrium, Phys. Rev. **40**, 749 (1932).
[56] H. J. Groenewold, On the principles of elementary quantum mechanics, Physica **12**, 405 (1946).
[57] J. E. Moyal, Quantum mechanics as a statistical theory, Proc. Cambridge Philos. Soc. **45**, 99 (1949).
[58] J. Schwinger, Unitary operator bases, Proc. Natl. Acad. Sci. U.S.A. **46**, 570 (1960).
[59] F. A. Buot, Method for calculating TrH^n in solid-state theory, Phys. Rev. B **10**, 3700 (1974).
[60] F. A. Buot, *Nonequilibrium Quantum Transport Physics in Nanosystems* (World Scientific, Singapore, 2009).
[61] F. A. Buot, Quantum superfield theory and lattice Weyl transform in nonequilibrium quantum transport physics, Quantum Matter **2**, 247 (2013).
[62] W. K. Wootters, A Wigner-function formulation of finite-state quantum mechanics, Ann. Phys. (N.Y.) **176**, 1 (1987).
[63] U. Leonhardt, Quantum-State Tomography and Discrete Wigner Function, Phys. Rev. Lett. **74**, 4101 (1995).
[64] P. Kasperkovitz and M. Peev, Wigner-Weyl formalisms for toroidal geometries, Ann. Phys. (N.Y.) **230**, 21 (1994).
[65] M. Ligabo, Torus as phase space: Weyl quantization, dequantization, and Wigner formalism, J. Math. Phys. (N.Y.) **57**, 082110 (2016).
[66] I. V. Fialkovsky and M. A. Zubkov, Precise Wigner-Weyl calculus for lattice models, Nucl. Phys. **B954**, 11499 (2020).
[67] C. Zhang and M. Zubkov, Note on the Bloch theorem, Phys. Rev. D **100**, 116021 (2019).
[68] M. Suleymanov and M. A. Zubkov, Wigner–Weyl formalism and the propagator of Wilson fermions in the presence of varying external electromagnetic field, Nucl. Phys. **B938**, 171 (2019).
[69] I. V. Fialkovsky and M. A. Zubkov, Elastic deformations and Wigner–Weyl formalism in graphene, Symmetry **12**, 317 (2020).
[70] C. Zhang and M. A. Zubkov, Hall conductivity as the topological invariant in the phase space in the presence of interactions and a nonuniform magnetic field, JETP Lett. **110**, 487 (2019).
[71] C. Zhang and M. A. Zubkov, Feynman rules in terms of the Wigner transformed Green functions, Phys. Lett. B **802**, 13519 (2020).
[72] G. E. Volovik, *The Universe in a Helium Droplet* (Clarendon Press Oxford, UK, 2003).
[73] Y. A. Simonov and J. A. Tjon, The Feynman-Schwinger (worldline) representation in perturbative QCD, in *Multiple Facets of Quantization and Supersymmetry* (World Scientific, Singapore, 2002).
[74] Y. A. Simonov and M. A. Trusov, Quarks and baryons in QCD at finite density, arXiv:0908.3276.
[75] R. A. Abramchuk, M. A. Andreichikov, Z. V. Khaidukov, and Y. A. Simonov, Dense quark–gluon plasma in strong magnetic fields, Eur. Phys. J. C **79**, 1040 (2019).
[76] V. D. Orlovsky and Y. A. Simonov, Quark-hadron thermodynamics in a magnetic field, Phys. Rev. D **89**, 054012 (2014).
[77] N. O. Agasian, M. S. Lukashov, and Y. A. Simonov, Nonperturbative SU(3) thermodynamics and the phase transition, Eur. Phys. J. A **53**, 138 (2017).
[78] M. A. Andreichikov, M. S. Lukashov, and Y. A. Simonov, Nonperturbative quark–gluon thermodynamics at finite density, Int. J. Mod. Phys. A **33**, 1850043 (2018).
[79] N. O. Agasian and Y. A. Simonov, New nonperturbative approach to the Debye mass in hot QCD, Phys. Lett. B **639**, 82 (2006).
[80] Y. A. Simonov, Magnetic confinement and the Linde problem, Phys. Rev. D **96**, 096002 (2017).
[81] C. Zhang and M. Zubkov, Influence of interactions on integer quantum Hall effect, Ann. Phys. (Amsterdam) **444**, 169016 (2022).
[82] M. A. Zubkov and X. Wu, Topological invariant in terms of the Green functions for the quantum Hall effect in the presence of varying magnetic field, Ann. Phys. (Amsterdam) **418**, 168179 (2020).
[83] R. Abramchuk (to be published).
[84] M. Zubkov, Abelian Fock—Schwinger representation for the quark propagator in external gauge field, Phys. Lett. B **810**, 135811 (2020).
[85] Y. A. Simonov, Nonperturbative corrections to the quark selfenergy, Phys. Lett. B **515**, 137 (2001).
[86] R. Abramchuk, Z. V. Khaidukov, and M. A. Zubkov, Anatomy of the chiral vortical effect, Phys. Rev. D **98**, 076013 (2018).
[87] D. fu Hou, H. Liu, and H. cang Ren, Possible higher order correction to the chiral vortical conductivity in a gauge field plasma, Phys. Rev. D **86**, 121703 (2012).
[88] S. Golkar and D. T. Son, (Non)-renormalization of the chiral vortical effect coefficient, J. High Energy Phys. 02 (2015) 196.
[89] M. L. Bellac, *Thermal Field Theory* Cambridge Monographs on Mathematical Physics (Cambridge University Press, Cambridge, England, 2011), p. 3.